

# Linear MHD stability studies with the STARWALL code

P. Merkel, and E. Strumberger  
Max Planck Institute for Plasma Physics, Boltzmannstr. 2.  
85748 Garching, Germany

August 21, 2015

## Abstract

The STARWALL/CAS3D/OPTIM code package is a powerful tool to study the linear MHD stability of 3D, ideal equilibria in the presence of multiply-connected ideal and/or resistive conducting structures, and their feedback stabilization by external currents. Robust feedback stabilization of resistive wall modes can be modelled with the OPTIM code. Resistive MHD studies are possible combining STARWALL with the linear, resistive 2D CASTOR code as well as nonlinear MHD simulations combining STARWALL with the JOEKE code.

In the present paper, a detailed description of the STARWALL code is given and some of its applications are presented to demonstrate the methods used. Conducting structures are treated in the thin wall approximation and depending on their complexity they are discretized by a spectral method or by triangular finite elements. As an example, a configuration is considered consisting of an ideal plasma surrounded by a vacuum domain containing a resistive wall and bounded by an external wall. Ideal linear MHD modes and resistive wall modes in the presence of multiply-connected walls are studied. In order to treat the vertical mode self-consistently the STARWALL code has been completed by adding the so-called Lüst-Martensen term generated by a constant normal displacement of the plasma.

The appendix contains the computation of the 2D Fourier transform of singular inductance integrals, and the derivation of an asymptotic expansion for large Fourier harmonics.

**Keywords:** resistive wall modes, vertical modes, energy principle, multiply-connected wall structures, variational method, finite element method

# 1 Introduction

The STARWALL code has originally been developed for the numerical treatment of resistive wall modes (RWMs). It has been applied to many different physics problems via a coupling to linear and non-linear MHD codes already (see also the outlook in Section 6). The present paper concentrates on STARWALL itself, in particular on the mathematical and numerical methods used.

After briefly introducing resistive wall modes, this introductory part explains the main features of the STARWALL code and its interaction with other codes. Feedback stabilization studies of RWMs are described, and the recently added Lüst-Martensen term which is important for axisymmetric instabilities is introduced. Finally the outline of the rest of the paper is given.

External kink unstable tokamak equilibria which are fully stabilized by an ideal conducting wall sufficiently close to the plasma remain unstable in the presence of a realistic wall because of its finite resistivity. These instabilities, Resistive Wall Modes (RWMs), grow on the time scale of the magnetic field diffusion through the resistive wall. With the growth rate of the RWM being typically orders of magnitude smaller than that of the kink mode in the absence of a wall, stabilizing the modes with an active feedback system becomes feasible. The topical review on stabilization of the external kink and the resistive wall mode by Chu and Okabayashi [1] gives a comprehensive overview of the existing literature on this topic.

Beside STARWALL – presented here – several other codes have been developed and used to study RWMs: VALEN [2, 3], DCON coupled to VACUUM [4], MARS-F [5], CarMa [6]. In the VALEN code the plasma state is approximated by a single unstable eigenfunction, whereas in MARS-F and CarMa the stability of 2D equilibria in the presence of 3D structures is treated. STARWALL is the only code which can be applied to 3D equilibria with general 3D wall configurations. Both, VALEN and STARWALL use a thin wall approximation.

The STARWALL code is part of a comprehensive code package: 3D equilibrium NEMEC code [7, 8, 9], coordinate transformation COTRANS code, 3D ideal MHD stability CAS3D code [10], vacuum and RWM stability STARWALL code, and the feedback optimization OPTIM code [11].

An adapted version of the STARWALL code has also been coupled [12] to the non-linear MHD code JOREK [13] to include resistive wall effects in the simulations and has already

been applied to a variety of different physics problems. The CASTOR3D code is currently under development [14], for linear stability studies of 3D equilibria including 3D resistive wall effects described in the STARWALL formalism. Some additional information on JOREK-STARWALL and CASTOR3D is provided in Section 6.

Computations of external modes with ideal conducting wall configurations are possible with the CAS3D code including the perturbed kinetic energy where the vacuum energy term is provided by the STARWALL code. In case of slowly growing resistive wall modes, the plasma inertia can be neglected such that a problem of first order in time is obtained [4]. These modes can be studied with the STARWALL code. Also, the feedback stabilization of RWMs can be investigated as described in the following. The feedback procedure can be divided in two parts, the open-loop and the closed-loop problem. In the open-loop part, a complete set of eigenfunctions of the plasma-resistive-wall system is determined. The feedback coils can be included in the resistive wall configuration passive resistive elements without external voltage applied.

The closed-loop part consists of feedback logics which calculate the optimal voltages to be applied at the feedback coils based on signals which are produced by sensor coils at appropriate positions. The feedback code OPTIM [11] implemented for this purpose achieves robust control by considering all unstable, but also a set of stable modes to assure that modes are not driven unstable by the active feedback.

RWM kink modes and their feedback stabilization have been studied for ITER and ASDEX Upgrade tokamak-type configurations with realistic wall structures and for 3D quasi-axisymmetric equilibria [15, 16, 17, 18, 19].

To study external axisymmetric modes (toroidal harmonic  $n = 0$ ) the STARWALL code has been completed by implementing the so-called Lüst-Martensen term [20]. The vacuum contribution of an external mode is determined by the normal displacement  $\xi_n$  at the plasma boundary. For  $\xi_n \neq const$  the vacuum contribution is the solution of a Neumann-type problem with prescribed normal component  $\mathbf{B}_n$ . The Lüst-Martensen term is the plasma perturbation for  $\xi_n = const$  where the perturbed  $\mathbf{B}_{vac}$  is tangential at the plasma boundary. In that case a net-toroidal and net-poloidal magnetic flux is induced in the vacuum region bounded by the plasma boundary and an external ideal conducting wall or at least by ideal toroidal field coils. That is, for vertical mode studies the identical physical configuration should be used by which the free-boundary equilibrium was generated. Results of Vertical Displacement Events (VDEs) taking into account the Lüst-Martensen term and their coupling to higher toroidal harmonics via a three-dimensional resistive wall are presented for an AUG-type configuration in Section 5.

The rest of this paper is organized as follows. In Section 2, the physical problem to be solved for vacuum, resistive wall, and ideal plasma is defined. In Section 3 the variational procedure to solve this problem using a spectral discretization is described, and in Section 4 the method used for triangular finite elements is introduced. Section 5 contains an example for applying STARWALL to realistic geometries: Linear stability is investigated for an ASDEX Upgrade-type configuration including a 3D resistive wall with holes. In Section 6, a brief outlook to future applications of the STARWALL code for linear and non-linear MHD problems is given.

In Appendix A the variational method is explained comprehensively, and Appendix B contains the definition of the inductance matrices. In Appendix C the subtraction method for the treatment of the singular matrix elements is described. Appendix D contains the computation of the 2D Fourier transform of singular inductance terms already published in [21] and [22]. The treatment of unstable recurrence relations by a method running the recursion in the backward direction has been added. Furthermore, the derivation of an asymptotic expansion for large values of the 2D Fourier harmonics  $m, n$  for the singular Fourier integrals is given.

## 2 The vacuum contribution

The STARWALL procedure will be explained considering an ideal plasma equilibrium in the presence of a multiply-connected resistive wall and an external ideal conducting (superconducting) wall (see Fig. 1 and Fig. 2). For the resistive wall the thin-wall approximation is used [23]. Assuming the RWM to be sufficiently slow, the kinetic energy of the plasma perturbation can be neglected. In analogy to the ideal energy principle [24] a variational technique can be applied. The Lagrangian

$$\mathcal{L} = W_p(\boldsymbol{\xi}, \boldsymbol{\xi}) + \frac{1}{2} \int_{S_1} df (\mathbf{n} \cdot \boldsymbol{\xi})(\mathbf{B} \cdot \mathbf{B}_0) \quad (1)$$

consists of the potential energy of the plasma perturbation and the contribution of the vacuum domain given by a surface integral at the plasma-vacuum interface ( $S_1 =$  plasma-vacuum interface,  $\boldsymbol{\xi} =$  displacement vector,  $\mathbf{B}_0 =$  equilibrium magnetic field,  $\mathbf{B} =$  perturbed vacuum magnetic field,  $\mathbf{n} =$  exterior normal on  $S_1$ ). The perturbed magnetic field  $\mathbf{B}$  is uniquely determined by the normal component  $\mathbf{n} \cdot \boldsymbol{\xi}$  of the displacement  $\boldsymbol{\xi}$  at  $S_1$ .

The potential energy of the plasma perturbation [25] - provided by the CAS3D code - is given by

$$\begin{aligned}
W_p(\boldsymbol{\xi}, \boldsymbol{\xi}) &= \frac{1}{2} \int_{S_1} d^3r [\mathbf{C}^2 + \Gamma p (\nabla \cdot \boldsymbol{\xi})^2 - \mathcal{A} (\boldsymbol{\xi} \cdot \mathbf{n})^2], \\
\mathbf{C} &= \nabla \times (\boldsymbol{\xi} \times \mathbf{B}_0) + (\boldsymbol{\xi} \cdot \mathbf{n}) \mathbf{j} \times \mathbf{n}, \quad \mathcal{A} = 2(\mathbf{j} \times \mathbf{n}) \cdot (\mathbf{B}_0 \cdot \nabla) \mathbf{n}, \\
\mathbf{B}_0 &= \nabla s \times \nabla (F'_P v - F'_T u),
\end{aligned} \tag{2}$$

where  $s, u, v$  are flux coordinates:  $s : 0 \leq s \leq 1$  is the normalized toroidal flux, and  $(u, v) : 0 \leq u, v \leq 1$  are poloidal and toroidal magnetic coordinates on the surfaces.  $F'_P, F'_T$  are the derivatives of the poloidal and toroidal flux with respect to  $s$ . The Fourier expansion of the displacement vector reads

$$\boldsymbol{\xi}(s, u, v) = \sum_{\substack{mf, nf \\ m=0, n=0 \\ m>0, n=-nf}} \boldsymbol{\xi}_s(s)_{mn} \sin 2\pi(mu + nv) + \boldsymbol{\xi}_c(s)_{mn} \cos 2\pi(mu + nv). \tag{3}$$

With respect to the flux coordinate  $s$ , the Fourier harmonics  $\boldsymbol{\xi}_s(s)_{mn}, \boldsymbol{\xi}_c(s)_{mn}$  are discretized using a finite element method.

The perturbed magnetic field  $\mathbf{B}$  has to satisfy Maxwell's equations

$$\mathbf{B} = \nabla \times \mathbf{A}, \quad \nabla \times (\nabla \times \mathbf{A}) = 0, \quad \nabla \cdot \mathbf{A} = 0 \tag{4}$$

with boundary conditions for the vector potential  $\mathbf{A}$  at the plasma-vacuum interface, the resistive wall and the external superconducting wall.

On the resistive wall the boundary condition follows from Faraday's and Ohm's law:  $\mathbf{E} + \frac{\partial \mathbf{A}}{\partial t} = 0$ ,  $\sigma \mathbf{E} = \mathbf{J}$ . Assuming a time dependence  $e^{\gamma t}$ , one gets in the thin wall approximation the boundary conditions for the perturbed vector potential

$$\mathbf{n} \times \mathbf{A} = \begin{cases} -(\mathbf{n} \cdot \boldsymbol{\xi}) \mathbf{B}_0 & : \text{ on } S_1 \text{ (plasma-vacuum interface)} \\ -\frac{1}{\sigma d} \mathbf{n} \times \mathbf{j}_2 & : \text{ on } S_2 \text{ (resistive wall)} \\ 0 & : \text{ on } S_3 \text{ (external conducting wall)} \end{cases} \tag{5}$$

where  $\mathbf{j}_2$  is the current in the resistive wall,  $\mathbf{n}$  is the exterior normal unit vector on the surfaces,  $\sigma d$  is the surface resistance of the wall ( $\sigma = \text{conductivity}$ ,  $d = \text{wall thickness}$ ) and  $\mathbf{B}_0$  is the equilibrium magnetic field.

With the contravariant normal component  $\nabla s \cdot \boldsymbol{\xi}$  used in the CAS3D code the boundary condition at the plasma-vacuum interface reads

$$\nabla s \times \mathbf{A} = -(\nabla s \cdot \boldsymbol{\xi}) \mathbf{B}_0, \quad \nabla s = \frac{|\mathbf{r}_v \times \mathbf{r}_u|}{(\mathbf{r}_v \times \mathbf{r}_u) \cdot \mathbf{r}_s} \mathbf{n}, \quad \mathbf{B}_0 = \frac{F'_T \mathbf{r}_v + F'_P \mathbf{r}_u}{(\mathbf{r}_v \times \mathbf{r}_u) \cdot \mathbf{r}_s} \tag{6}$$

with the equilibrium field  $\mathbf{B}_0$  in magnetic coordinates and  $\mathbf{r}_u := \frac{\partial \mathbf{r}}{\partial u}$ ,  $\mathbf{r}_v := \frac{\partial \mathbf{r}}{\partial v}$ ,  $\mathbf{r}_s := \frac{\partial \mathbf{r}}{\partial s}$ .

Multiplying (5) with  $\mathbf{n} \times \mathbf{r}_u$  and  $\mathbf{n} \times \mathbf{r}_v$  one gets

$$\begin{aligned} \mathbf{r}_{1,u} \cdot \mathbf{A} &= F'_T \nabla s \cdot \boldsymbol{\xi}, & \mathbf{r}_{1,v} \cdot \mathbf{A} &= -F'_P \nabla s \cdot \boldsymbol{\xi} & : & \text{on } S_1 \\ \mathbf{r}_{2,u} \cdot \mathbf{A} &= -\frac{1}{\sigma d\gamma} \mathbf{r}_{2,u} \cdot \mathbf{j}_2, & \mathbf{r}_{2,v} \cdot \mathbf{A} &= -\frac{1}{\sigma d\gamma} \mathbf{r}_{2,v} \cdot \mathbf{j}_2 & : & \text{on } S_2 \\ \mathbf{r}_{3,u} \cdot \mathbf{A} &= 0, & \mathbf{r}_{3,v} \cdot \mathbf{A} &= 0 & : & \text{on } S_3 \end{aligned} \quad (7)$$

The boundary conditions for the perturbed magnetic field  $\mathbf{B}$  are obtained by taking the divergence:  $[\nabla \cdot (\nabla s \times \mathbf{A}) = \mathbf{A} \cdot (\nabla \times \nabla s) - \nabla s \cdot \mathbf{B}]$ . At the plasma-vacuum interface  $S_1$  one gets

$$\nabla s \cdot \mathbf{B} = \mathbf{B}_0 \cdot \nabla (\nabla s \cdot \boldsymbol{\xi}) \quad (8)$$

or

$$\mathbf{N} \cdot \mathbf{B} = \begin{cases} F'_T (\nabla s \cdot \boldsymbol{\xi})_v + F'_P (\nabla s \cdot \boldsymbol{\xi})_u & : \text{ on } S_1 \text{ (plasma-vacuum interface)} \\ \frac{1}{\sigma d\gamma} (\mathbf{r}_{2,v} \cdot \mathbf{j}_{2,u} - \mathbf{r}_{2,u} \cdot \mathbf{j}_{2,v}) & : \text{ on } S_2 \text{ (resistive wall)} \\ 0 & : \text{ on } S_3 \text{ (external conducting wall)} \end{cases} \quad (9)$$

with  $\mathbf{N} = \mathbf{r}_v \times \mathbf{r}_u$  to be taken at the surfaces.

Prescribing the normal component  $\nabla s \cdot \mathbf{B}$  of  $\mathbf{B}$  one has to solve a Neumann-type problem except for  $\nabla s \cdot \boldsymbol{\xi} = \text{constant}$  where the normal component of  $\mathbf{B}$  vanishes. To get the boundary condition for this case one has to go back to the boundary condition for the vector potential  $\mathbf{A}$ .

The solution for the vector potential  $\mathbf{A}$  can be generated by surface currents on the plasma-vacuum interface  $S_1$ , the resistive wall  $S_2$  and the external ideal conducting wall  $S_3$

$$\mathbf{A}(\mathbf{r}) = \frac{1}{4\pi} \sum_{i=1}^3 \int_{S_i} df_i \frac{\mathbf{j}_i}{|\mathbf{r} - \mathbf{r}_i|} \quad (10)$$

with divergence-free surface currents derived from current potentials  $\Phi_i$

$$\mathbf{j}_i = \mathbf{n}_i \times \nabla \Phi_i, \quad \mathbf{n}_i = \frac{\mathbf{r}_{i,v} \times \mathbf{r}_{i,u}}{|\mathbf{r}_{i,v} \times \mathbf{r}_{i,u}|}, \quad i = 1, 2, 3 \quad (11)$$

where  $\mathbf{n}_i$ ,  $i = 1, 2, 3$  are the exterior unit normal vectors.

For toroidally and poloidally closed tori the current potential is given by

$$\Phi_i = I_i^T u + I_i^P v + \phi_i(u, v), \quad i = 1, 2, 3 \quad (12)$$

where  $I_i^T, I_i^P$  are net-toroidal and net-poloidal currents on the torus. They play a role only if the displacement  $\boldsymbol{\xi}$  contains a component  $\nabla s \cdot \boldsymbol{\xi} = \text{constant}$  [20]. The  $\phi_i(u, v)$  are single-valued potentials which can be expanded in Fourier space for smooth tori

$$\phi_i(u, v) = \sum_{\substack{m=0, n=1 \\ m>0, n=-n_c}}^{m_c, n_c} \hat{\phi}_i^s(m, n) \sin 2\pi(mu + nv) + \hat{\phi}_i^c(m, n) \cos 2\pi(mu + nv), \quad i = 1, 2, 3 \quad (13)$$

The surface currents have to be determined such that the boundary conditions for  $\mathbf{A}$  on  $S_i$ ,  $i=1,2,3$  are satisfied. That will be carried out by means of a variational procedure.

### 3 Variational method

To treat cases with multiply-connected resistive wall configurations, a finite element method has been applied using a variational procedure [23]. One introduces the Lagrangian

$$\mathcal{L}_V = \frac{1}{8\pi} \sum_{i=1}^3 \sum_{k=1}^3 \int_{S_i} df_i \int_{S_k} df_k \frac{\mathbf{j}_i \cdot \mathbf{j}_k}{|\mathbf{r}_i - \mathbf{r}_k|} + \frac{1}{2\gamma} \int_{S_2} df_2 \frac{\mathbf{j}_2 \cdot \mathbf{j}_2}{\sigma d} + \int_{S_1} df_1 (\mathbf{n}_1 \cdot \boldsymbol{\xi}) \mathbf{n}_1 \cdot (\mathbf{j}_1 \times \mathbf{B}_0) \quad (14)$$

In appendix A it is shown that the first variation  $\delta\mathcal{L}_V = 0$  gives the boundary conditions (A.10),(A.11),(A.12). Assuming a smooth plasma-vacuum interface being identical with the plasma boundary the current potential and the normal component of the displacement vector can be expanded in Fourier space

$$\boldsymbol{\xi} \cdot \nabla s = \sum_{\substack{m=0, n=0 \\ m>0, n=-n_f}}^{m_f, n_f} \hat{\xi}_s(m, n) \sin 2\pi(mu + nv) + \hat{\xi}_c(m, n) \cos 2\pi(mu + nv) \quad (15)$$

so that one gets for the last term of the Lagrangian  $\mathcal{L}_V$

$$\begin{aligned} \int_{S_1} df_1 (\mathbf{n}_1 \cdot \boldsymbol{\xi}) \mathbf{n}_1 \cdot (\mathbf{j}_1 \times \mathbf{B}_0) &= -(F_T' I_1^P + F_P' I_1^T) \hat{\xi}_c(0, 0) \\ &+ \sum_{\substack{m=0, n=1 \\ m>0, n=-n_f}}^{m_f, n_f} \pi(nF_T' + mF_P') (\hat{\xi}_s(m, n) \hat{\phi}_1^c(m, n) - \hat{\xi}_c(m, n) \hat{\phi}_1^s(m, n)) \end{aligned} \quad (16)$$

being linear in  $\Phi_1$  and determining the boundary condition at the plasma-vacuum interface. The variables of the Lagrangian  $\mathcal{L}_V$  are the net-currents  $I_i^T, I_i^P$  and the Fourier

harmonics of the single-valued potentials  $\hat{\phi}_i, i = 1, 2, 3$ . Replacing in  $\mathcal{L}_V$  the currents using (11) one gets

$$\mathcal{L}_V = \frac{1}{2} \sum_{i=1}^3 \sum_{k=1}^3 \hat{\Phi}_i^\top \mathbf{M}_{ik} \hat{\Phi}_k + \frac{1}{2\gamma} \hat{\Phi}_2^\top \mathbf{N}_{22} \hat{\Phi}_2 + \hat{\Phi}_1^\top \mathbf{M}_{1\xi} \hat{\xi} \quad (17)$$

with

$$\begin{aligned} \hat{\Phi}_i^\top &= [I_i^T, I_i^P, \hat{\phi}_i^s(0, 1), \dots, \hat{\phi}_i^s(m_{f_i}, n_{f_i}), \hat{\phi}_i^c(0, 1), \dots, \hat{\phi}_i^c(m_{f_i}, n_{f_i})] \\ \hat{\xi}^\top &= [\hat{\xi}_s(0, 1), \dots, \hat{\xi}_s(m_f, n_f), \hat{\xi}_c(0, 0), \dots, \hat{\xi}_c(m_f, n_f)] \end{aligned} \quad (18)$$

and  $\top \equiv$  transpose.

Varying  $\mathcal{L}_V$  with respect to  $\hat{\Phi}_i, i = 1, 2, 3$  one gets a set of linear equations for  $\hat{\Phi}_i$ .

$$\begin{aligned} \mathbf{M}_{pp} \hat{\Phi}_p + \mathbf{M}_{pw} \hat{\Phi}_w + \mathbf{M}_{pt} \hat{\Phi}_t &= -\mathbf{M}_{p\xi} \hat{\xi} \\ \mathbf{M}_{wp} \hat{\Phi}_p + \mathbf{M}_{ww} \hat{\Phi}_w + \mathbf{M}_{wt} \hat{\Phi}_t &= 0, \\ \mathbf{M}_{tp} \hat{\Phi}_p + \mathbf{M}_{tw} \hat{\Phi}_w + \mathbf{M}_{tt} \hat{\Phi}_t &= -\frac{1}{\gamma} \mathbf{N}_{tt} \hat{\Phi}_t \end{aligned} \quad (19)$$

(note: the index notation has been changed  $p \equiv 1$  - plasma-vacuum interface,  $t \equiv 2$  - resistive wall,  $w \equiv 3$  - external conducting wall)

The vacuum contribution in (1) is given by

$$W_s = \frac{1}{2} \int_{S_1} du dv (\boldsymbol{\xi} \cdot \nabla s) (F'_P \mathbf{r}_{1,u} + F'_T \mathbf{r}_{1,v}) \cdot \mathbf{B} \quad (20)$$

with the magnetic field generated by the currents on the surfaces  $S_i, i = 1, 2, 3$

$$\mathbf{B}(\mathbf{r}) = \frac{1}{4\pi} \sum_{i=1}^3 \left[ \int_{S_i} du' dv' \frac{(I_i^P \mathbf{r}_{i,u'} - I_i^T \mathbf{r}_{i,v'}) \times (\mathbf{r} - \mathbf{r}'_i)}{|\mathbf{r} - \mathbf{r}'_i|^3} + \nabla \int_{S_i} (d\mathbf{f}' \cdot \nabla' \frac{1}{|\mathbf{r} - \mathbf{r}'_i|}) \phi'_i \right] \quad (21)$$

Inserting (21) into (20),  $W_s$  splits into two terms

$$W_s = \frac{1}{2} \sum_{i=1}^3 (W_i^{(1)} + W_i^{(2)}) \quad (22)$$

The contributions for  $i = 1$  are given by

$$\begin{aligned} W_1^{(1)} &= \frac{1}{4\pi} \int_{S_1} du dv (\boldsymbol{\xi} \cdot \nabla s) \left( \int_{S_1} du' dv' (F'_P \mathbf{r}_{1,u} + F'_T \mathbf{r}_{1,v}) \times (I_1^P \mathbf{r}_{1,u'} - I_1^T \mathbf{r}_{1,v'}) \cdot \frac{(\mathbf{r}_1 - \mathbf{r}'_1)}{|\mathbf{r}_1 - \mathbf{r}'_1|^3} \right. \\ &\quad \left. + 2\pi (F'_P I_1^T + F'_T I_1^P) \right) \\ W_1^{(2)} &= -\frac{1}{4\pi} \int_{S_1} du dv \left[ (F'_P \frac{\partial}{\partial u} + F'_T \frac{\partial}{\partial v}) (\boldsymbol{\xi} \cdot \nabla s) \right] \left( 2\pi \phi(u, v) \right. \\ &\quad \left. + \int_{S_1} du' dv' (\mathbf{r}_{1,v'} \times \mathbf{r}_{1,u'}) \cdot \frac{(\mathbf{r}_1 - \mathbf{r}'_1)}{|\mathbf{r}_1 - \mathbf{r}'_1|^3} \phi_1(u', v') \right) \end{aligned} \quad (23)$$



For  $i = 2, 3$  the contributions to (22) are given by

$$\begin{aligned} W_i^{(1)} &= \frac{1}{4\pi} \int_{S_1} du dv (\boldsymbol{\xi} \cdot \nabla s) \int_{S_i} du' dv' (F'_P \mathbf{r}_{1,u} + F'_T \mathbf{r}_{1,v}) \times (I_i^P \mathbf{r}_{i,u'} - I_i^T \mathbf{r}_{i,v'}) \cdot \frac{(\mathbf{r}_1 - \mathbf{r}'_i)}{|\mathbf{r}_1 - \mathbf{r}'_i|^3} \\ W_i^{(2)} &= \frac{-1}{4\pi} \int_{S_1} du dv \left[ (F'_P \frac{\partial}{\partial u} + F'_T \frac{\partial}{\partial v}) (\boldsymbol{\xi} \cdot \nabla s) \right] \int_{S_i} du' dv' (\mathbf{r}_{i,v'} \times \mathbf{r}_{i,u'}) \cdot \frac{(\mathbf{r}_1 - \mathbf{r}'_i)}{|\mathbf{r}_1 - \mathbf{r}'_i|^3} \phi'_i \end{aligned} \quad (24)$$

The  $u, v$ -integrations have to be performed infinitesimal exterior of the plasma-vacuum interface  $S_1$  and the singular integrals  $W_1^{(1)}, W_1^{(2)}$  are treated using a subtraction method (see appendix B).

With the definitions (18) the vacuum contribution  $W_s$  reads

$$W_s = \frac{1}{2} (\hat{\xi}^\top \mathbf{M}_{\hat{\xi}p} \hat{\Phi}_p + \hat{\xi}^\top \mathbf{M}_{\hat{\xi}w} \hat{\Phi}_w + \hat{\xi}^\top \mathbf{M}_{\hat{\xi}t} \hat{\Phi}_t) \quad (25)$$

The elements of the matrices  $\mathbf{M}_{\hat{\xi}p}, \mathbf{M}_{\hat{\xi}w}$  and  $\mathbf{M}_{\hat{\xi}t}$  are given in appendix B.

The variables of the system considered are the Fourier harmonics of the displacement vector  $\boldsymbol{\xi}$ , the current potentials on the plasma-vacuum interface, the resistive wall and the external wall. The set of equations (19) determines the current potentials for given normal component  $\hat{\xi}$  of the displacement vector on the plasma-vacuum interface.

The system is closed by the equation derived from the Lagrangian (1). Varying the discretized functional (1) one obtains

$$\begin{pmatrix} \mathbf{M}_{XX} & \mathbf{M}_{X\hat{\xi}} \\ \mathbf{M}_{\hat{\xi}X} & \mathbf{M}_{\hat{\xi}\hat{\xi}} \end{pmatrix} \cdot \begin{pmatrix} X \\ \hat{\xi} \end{pmatrix} - \begin{pmatrix} 0 \\ \mathbf{M}_{\hat{\xi}p} \hat{\Phi}_p + \mathbf{M}_{\hat{\xi}w} \hat{\Phi}_w + \mathbf{M}_{\hat{\xi}t} \hat{\Phi}_t \end{pmatrix} = 0. \quad (26)$$

The variables are denoted as follows:  $X = \{\boldsymbol{\xi}_s(s_i)_{mn}, \dots, \boldsymbol{\xi}_c(s_i)_{mn}, \dots\}$  consists of all components of the displacement vector except for the Fourier harmonics of the normal component at the plasma boundary which are denoted by  $\hat{\xi} = \{\nabla s \cdot \boldsymbol{\xi}_s(1)_{mn}, \dots, \nabla s \cdot \boldsymbol{\xi}_c(1)_{mn}, \dots\}$ .

Solving the set of equations for  $\hat{\xi}$  one gets

$$\hat{\xi} = \overset{cas3d}{\mathbf{M}_{\hat{\xi}\hat{\xi}}} (\mathbf{M}_{\hat{\xi}p} \hat{\Phi}_p + \mathbf{M}_{\hat{\xi}w} \hat{\Phi}_w + \mathbf{M}_{\hat{\xi}t} \hat{\Phi}_t) \quad (27)$$

with

$$\overset{cas3d}{\mathbf{M}_{\hat{\xi}\hat{\xi}}} = (\mathbf{M}_{\hat{\xi}\hat{\xi}} - \mathbf{M}_{\hat{\xi}X} \mathbf{M}_{XX}^{-1} \mathbf{M}_{X\hat{\xi}})^{-1} \quad (28)$$

Eliminating  $\hat{\xi}$  in (19) one obtains

$$\begin{aligned}
\widetilde{\mathbf{M}}_{pp} \Phi_p + \widetilde{\mathbf{M}}_{pw} \Phi_w + \widetilde{\mathbf{M}}_{pt} \Phi_t &= 0, \\
\mathbf{M}_{wp} \hat{\Phi}_p + \mathbf{M}_{ww} \hat{\Phi}_w + \mathbf{M}_{wt} \hat{\Phi}_t &= 0, \\
\mathbf{M}_{tp} \hat{\Phi}_p + \mathbf{M}_{tw} \hat{\Phi}_w + \mathbf{M}_{tt} \hat{\Phi}_t &= -\frac{1}{\sigma d \gamma} \mathbf{N}_{tt} \hat{\Phi}_t.
\end{aligned} \tag{29}$$

with

$$\begin{aligned}
\widetilde{\mathbf{M}}_{pp} &= (\mathbf{M}_{pp} + \mathbf{M}_{p\hat{\xi}} \overset{cas3d}{\mathbf{M}}_{\hat{\xi}\hat{\xi}} \mathbf{M}_{\hat{\xi}p}) \\
\widetilde{\mathbf{M}}_{pw} &= (\mathbf{M}_{pw} + \mathbf{M}_{p\hat{\xi}} \overset{cas3d}{\mathbf{M}}_{\hat{\xi}\hat{\xi}} \mathbf{M}_{\hat{\xi}w}) \\
\widetilde{\mathbf{M}}_{pt} &= (\mathbf{M}_{pt} + \mathbf{M}_{p\hat{\xi}} \overset{cas3d}{\mathbf{M}}_{\hat{\xi}\hat{\xi}} \mathbf{M}_{\hat{\xi}t})
\end{aligned} \tag{30}$$

Finally one gets a set of linear equations defining an initial value problem of first order in time. Assuming a time dependence  $e^{\gamma t}$ , the normal modes of the system are obtained by solving the generalized eigenvalue problem

$$\gamma \left[ \mathbf{M}_{tt} - \begin{pmatrix} \mathbf{M}_{tp} & \mathbf{M}_{tw} \end{pmatrix} \begin{pmatrix} \widetilde{\mathbf{M}}_{pp} & \widetilde{\mathbf{M}}_{pw} \\ \mathbf{M}_{wp} & \mathbf{M}_{ww} \end{pmatrix}^{-1} \begin{pmatrix} \widetilde{\mathbf{M}}_{pt} \\ \mathbf{M}_{wt} \end{pmatrix} \right] \hat{\Phi}_t = -\frac{1}{\sigma d} \mathbf{N}_{tt} \hat{\Phi}_t \tag{31}$$

## 4 The finite element method

For the finite element procedure the conducting wall is discretized into triangles. The position vector of a triangle is given by

$$\mathbf{r} = \mathbf{r}_1 + \alpha \mathbf{r}_{2,1} + \beta \mathbf{r}_{3,1}, \quad \alpha \geq 0, \quad \beta \geq 0, \quad 0 \leq \alpha + \beta \leq 1, \quad \mathbf{r}_{i,k} = \mathbf{r}_i - \mathbf{r}_k, \quad i, k = 1, 2, 3 \tag{32}$$

with the vertices numbered anti-clockwise  $(\mathbf{r}_1, \mathbf{r}_2, \mathbf{r}_3)$  and  $\mathbf{r}_4 \equiv \mathbf{r}_1$ .

Assuming the surface-current density to be constant on the triangle the current can be written as

$$\mathbf{j}_{\Delta} = \frac{\phi_1 \mathbf{r}_{2,3} + \phi_2 \mathbf{r}_{3,1} + \phi_3 \mathbf{r}_{1,2}}{|\mathbf{r}_{2,1} \times \mathbf{r}_{3,2}|} \quad \text{or} \quad \mathbf{j}_{\Delta} = \sum_{i=1}^3 \phi_i \mathbf{e}_i, \quad \mathbf{e}_i = \frac{1}{2} \varepsilon_{ikl} \frac{\mathbf{r}_{k,l}}{|\mathbf{r}_{2,1} \times \mathbf{r}_{3,2}|} \tag{33}$$

where the  $\phi_i$  are the values of the current potential at the vertices of the triangles.

The contribution of a pair of triangles to the functional  $\mathcal{L}$  is given by

$$\mathcal{L}_{\Delta'\Delta} = \mathbf{j}_{\Delta'} \cdot \mathbf{j}_{\Delta} \frac{1}{8\pi} \int_{\Delta'} df' \int_{\Delta} df \frac{1}{|\mathbf{r}' - \mathbf{r}|} \tag{34}$$

$$\mathcal{L}_{\Delta'\Delta} = \frac{1}{2} \sum_{i,k=1}^3 \phi'_i L_{ik} \phi_k, \quad L_{ik} = \mathbf{e}'_i \cdot \mathbf{e}_k \frac{1}{4\pi} \int_{\Delta'} df' \int_{\Delta} df \frac{1}{|\mathbf{r}' - \mathbf{r}|}$$

The fourfold integral  $L_{i,k}$  can be computed analytically. One gets a sufficiently good approximation by performing two integrations analytically and the remaining two integrations numerically:

One obtains for the twofold integral

$$\int_{\Delta'} df' \frac{1}{|\mathbf{r} - \mathbf{r}'|} = \sum_{i=1}^3 |\mathbf{r}_{i+1,i}| \left( a_i \ln \frac{l_i^+ + l_i^- + 1}{l_i^+ + l_i^- - 1} - h_i \left( \arctan \frac{a_i d_i^+}{a_i^2 + h_i^2 + l_i^+ h_i} - \arctan \frac{a_i d_i^-}{a_i^2 + h_i^2 + l_i^- h_i} \right) \right) \quad (35)$$

with

$$l_i^+ = \frac{|\mathbf{r}_{i+1} - \mathbf{r}|}{|\mathbf{r}_{i+1,i}|}, \quad l_i^- = \frac{|\mathbf{r}_i - \mathbf{r}|}{|\mathbf{r}_{i+1,i}|}, \quad d_i^+ = \frac{(\mathbf{r}_{i+1} - \mathbf{r}) \cdot \mathbf{r}_{i+1,i}}{|\mathbf{r}_{i+1,i}|^2}, \quad d_i^- = \frac{(\mathbf{r}_i - \mathbf{r}) \cdot \mathbf{r}_{i+1,i}}{|\mathbf{r}_{i+1,i}|^2}$$

$$a_i = \frac{(\mathbf{r}_i - \mathbf{r}) \times \mathbf{r}_{i+1,i} \cdot \mathbf{n}}{|\mathbf{r}_{i+1,i}|^2}, \quad h_i = \frac{|(\mathbf{r}_i - \mathbf{r}) \cdot \mathbf{n}|}{|\mathbf{r}_{i+1,i}|}, \quad \mathbf{n} = \frac{\mathbf{r}_{2,1} \times \mathbf{r}_{3,1}}{|\mathbf{r}_{2,1} \times \mathbf{r}_{3,1}|}$$

The remaining two integrations are done numerically using a  $N_g = 3$ -point or  $N_g = 7$ -point Gauss quadrature formula for a triangle domain

$$\int_{\Delta} df \int_{\Delta'} df' \frac{1}{|\mathbf{r} - \mathbf{r}'|} = \sum_{i=1}^{N_g} w_i \int_{\Delta'} df' \frac{1}{|\mathbf{r}_1 + \mathbf{r}_{2,1} \zeta_i + \mathbf{r}_{3,1} \eta_i - \mathbf{r}'|} \quad (36)$$

with  $\zeta_i$ ,  $\eta_i$ , and  $w_i$  listed in Table I.

$i$	$\zeta_i$	$\eta_i$	$w_i$
1	1/3	1/3	270/2400
2	$(6 + \sqrt{15})/21$	$(6 + \sqrt{15})/21$	$(155 + \sqrt{15})/2400$
3	$(9 - 2\sqrt{15})/21$	$(6 + \sqrt{15})/21$	$(155 + \sqrt{15})/2400$
4	$(6 + \sqrt{15})/21$	$(9 - 2\sqrt{15})/21$	$(155 + \sqrt{15})/2400$
5	$(6 - \sqrt{15})/21$	$(6 - \sqrt{15})/21$	$(155 - \sqrt{15})/2400$
6	$(9 + 2\sqrt{15})/21$	$(6 - \sqrt{15})/21$	$(155 - \sqrt{15})/2400$
7	$(6 - \sqrt{15})/21$	$(9 + 2\sqrt{15})/21$	$(155 - \sqrt{15})/2400$

(a)

$i$	$\zeta_i$	$\eta_i$	$w_i$
1	1/6	1/6	1/6
2	2/3	1/6	1/6
3	1/6	2/3	1/6

(b)

**Table I** Gauss quadrature with weights  $w_i$  at points  $\zeta_i$  and  $\eta_i$  for a  $N_g = 7$  point (a) and  $N_g = 3$  point (b) formula

For the self-inductance of a triangle one gets

$$L_{ik} = \mathbf{e}_i \cdot \mathbf{e}_k \frac{|\mathbf{r}_{2,1} \times \mathbf{r}_{3,1}|^2}{12\pi} \sum_{j=1}^3 \frac{1}{|\mathbf{r}_{j+1,j}|} \ln\left(\frac{L}{L - 2|\mathbf{r}_{j+1,j}|\right)} \quad (37)$$

with  $L = |\mathbf{r}_{2,1}| + |\mathbf{r}_{3,2}| + |\mathbf{r}_{1,3}|$ .

The magnetic field  $\mathbf{B}_\Delta$  produced by a constant current  $\mathbf{j}_\Delta$  on the triangle can be computed analytically

$$\mathbf{B}_\Delta = -\frac{1}{4\pi} \mathbf{j}_\Delta \times \nabla \int_{\Delta'} df' \frac{1}{|\mathbf{r} - \mathbf{r}'|} \quad (38)$$

with

$$\begin{aligned} \nabla \int_{\Delta'} df' \frac{1}{|\mathbf{r} - \mathbf{r}'|} &= \sum_{i=1}^3 \left( \frac{\mathbf{n} \times \mathbf{r}_{i+1,i}}{|\mathbf{r}_{i+1,i}|} \ln \frac{l_i^+ + l_i^- + 1}{l_i^+ + l_i^- - 1} \right. \\ &\quad \left. + \mathbf{n} \frac{(\mathbf{r}_i - \mathbf{r}) \cdot \mathbf{n}}{|(\mathbf{r}_i - \mathbf{r}) \cdot \mathbf{n}|} \left( \arctan \frac{a_i d_i^+}{a_i^2 + h_i^2 + l_i^+ h_i} - \arctan \frac{a_i d_i^-}{a_i^2 + h_i^2 + l_i^- h_i} \right) \right) \end{aligned} \quad (39)$$

so that the contribution of a triangle to the vacuum energy term (20) is given by

$$W_\Delta = \frac{1}{2} \int_{S_1} du dv (\nabla s \cdot \boldsymbol{\xi}) (F'_T \mathbf{r}_{1,v} + F'_P \mathbf{r}_{1,u}) \cdot \mathbf{B}_\Delta \quad (40)$$

The surface-current potential on a poloidally and toroidally closed surface consists of two multivalued secular terms determining the net-poloidal and net-toroidal current and of a single-valued periodic term  $\phi$ . The current potential is approximated by its value at the numbered global nodes of the triangulated domain. There are three local nodes at the vertices of each triangle. The nodes are numbered anti-clockwise. One defines the vector of the nodal values at the vertices of all triangles by

$$\bar{\Phi}(i) = U(i) I^T + V(i) I^P + \sum_{j=1}^{N_{ind}} \mathbf{H}(i, j) \phi(j), \quad i = 1, \dots, 3N_t \quad (41)$$

where  $N_t$  is the number of triangles and  $N_{ind}$  is the number of independent variables  $\phi(j)$  at the global nodes. A global node belongs to several triangles.  $U(i)$  and  $V(i)$  are the nodal values of a unit net-toroidal and net-poloidal current distribution which can be arbitrarily chosen. The so-called connectivity matrix  $\mathbf{H}$  relates the global nodes to the local nodes of the triangles. If there are holes in the wall the current potential has to satisfy the boundary condition  $\Phi = const.$  along the edges: the nodes at the vertices of the triangles along the edges of a hole have the same value reducing the number of the independent variables. That has to be incorporated in the connectivity matrix.

The matrix elements of a Lagrangian  $\mathcal{L}_S = \frac{1}{2}\bar{\Phi}^\top \bar{\mathbf{M}} \bar{\Phi}$  are

$$\bar{\mathbf{M}}_{3i-3+k, 3i'-3+k'} = \frac{\mathbf{e}_k^i \cdot \mathbf{e}_{k'}^{i'}}{4\pi} \int_{\Delta'} df' \int_{\Delta} df \frac{1}{|\mathbf{r}_{i'} - \mathbf{r}_i|}, \begin{cases} k = 1, 2, 3, & i = 1, \dots, N_t \\ k' = 1, 2, 3, & i' = 1, \dots, N_t \end{cases} \quad (42)$$

The contribution of a triangulated (resistive) wall to the Lagrangian is then given by

$$\mathcal{L}_S = \frac{1}{2}\Phi^\top \mathbf{M}_{tt} \Phi, \quad \mathbf{M}_{tt} = \mathbf{G}^\top \bar{\mathbf{M}} \mathbf{G}, \quad \mathbf{G} = (U, V, \mathbf{H}), \quad \Phi = \begin{pmatrix} I^T \\ I^P \\ \phi \end{pmatrix}, \quad (43)$$

where  $\Phi$  is the vector of the current potential of the independent variables. The contribution to the vacuum energy matrix of the wall is obtained with (38),(39),(42) and (43).

$$\mathbf{M}_{\xi t} = \bar{\mathbf{M}}_{\xi \bar{\Phi}} \mathbf{G}, \quad (44)$$

where the matrix elements of  $\bar{\mathbf{M}}_{\xi \bar{\Phi}}$  are the contributions to the Fourier harmonics of  $\nabla s \cdot \xi$  for the nodal values of the vertices of all triangles.

One possible choice for the net-current contribution for a closed torus without holes can be defined as follows: On a rectangular mesh with  $n_u$  poloidal and  $n_v$  toroidal meshpoints

$$(u_i, v_k) = \left( \frac{i-1}{n_u}, \frac{k-1}{n_v} \right), \quad \begin{matrix} i = 1, \dots, n_u + 1 \\ k = 1, \dots, n_v + 1 \end{matrix} \quad (45)$$

the positions of the  $2n_u n_v$  triangles are given by

$$\begin{aligned} \bar{\mathbf{r}}_{l-1,1} &= \mathbf{r}(u_i, v_{k+1}), \quad \bar{\mathbf{r}}_{l,1} = \mathbf{r}(u_{i+1}, v_k), \\ \bar{\mathbf{r}}_{l-1,2} &= \mathbf{r}(u_{i+1}, v_{k+1}), \quad \bar{\mathbf{r}}_{l,2} = \mathbf{r}(u_i, v_k), \quad l = 2(i + n_u(k-1)), \\ \bar{\mathbf{r}}_{l-1,3} &= \mathbf{r}(u_i, v_k), \quad \bar{\mathbf{r}}_{l,3} = \mathbf{r}(u_{i+1}, v_{k+1}) \end{aligned} \quad (46)$$

where  $l$  labels the triangles. There are  $(n_u + 1)(n_v + 1)$  nodes for the secular terms being proportional to  $I^T$  and  $I^P$ . The values of these current potential terms at the nodes can be chosen as

$$\begin{aligned} U(j) &= u_i, & j &= i + (n_u + 1)(k - 1), & i &= 1, \dots, n_u + 1 \\ V(j) &= v_k, & & & k &= 1, \dots, n_v + 1 \end{aligned} \quad (47)$$

while there are  $n_u n_v$  nodes for the periodic current potential  $\phi$ .

A resistive wall closed only poloidally or toroidally is topologically a cylinder. In that case the current potential becomes single-valued. For a poloidally (toroidally) closed wall the net-toroidal (net-poloidal) current vanishes and the net-poloidal (net-toroidal) current is given by the difference of the current potential value at the two boundaries of the wall.

## 5 Application

Numerical results are presented for an ASDEX Upgrade-type test equilibrium which is unstable with respect to external modes. The plasma equilibrium properties are: major radius  $R_0 = 1.64$  m, plasma current  $I_p = 0.98$  MA, monotone  $q$ -profile with  $q_{axis} = 1.46$  and  $q_{boundary} = 5.26$ , vacuum magnetic field strength  $B_0(R_0) = 2.43$  T, and volume average beta  $\langle \beta \rangle = 2.58\%$ . A poloidal cross-section of the flux surfaces, as well as the pressure and  $q$ -profiles are shown in Figs 1a-c. In Fig. 1a the positions of the plasma boundary (red), the resistive wall (blue), and the toroidal field coils (brown) are sketched. At the low field side the plasma boundary extends to  $R \approx 2.14$  m, while the resistive wall is localized at  $R \approx 2.23$  m, so that the plasma-wall distance amounts to  $\Delta R \approx 9$  cm at this position.

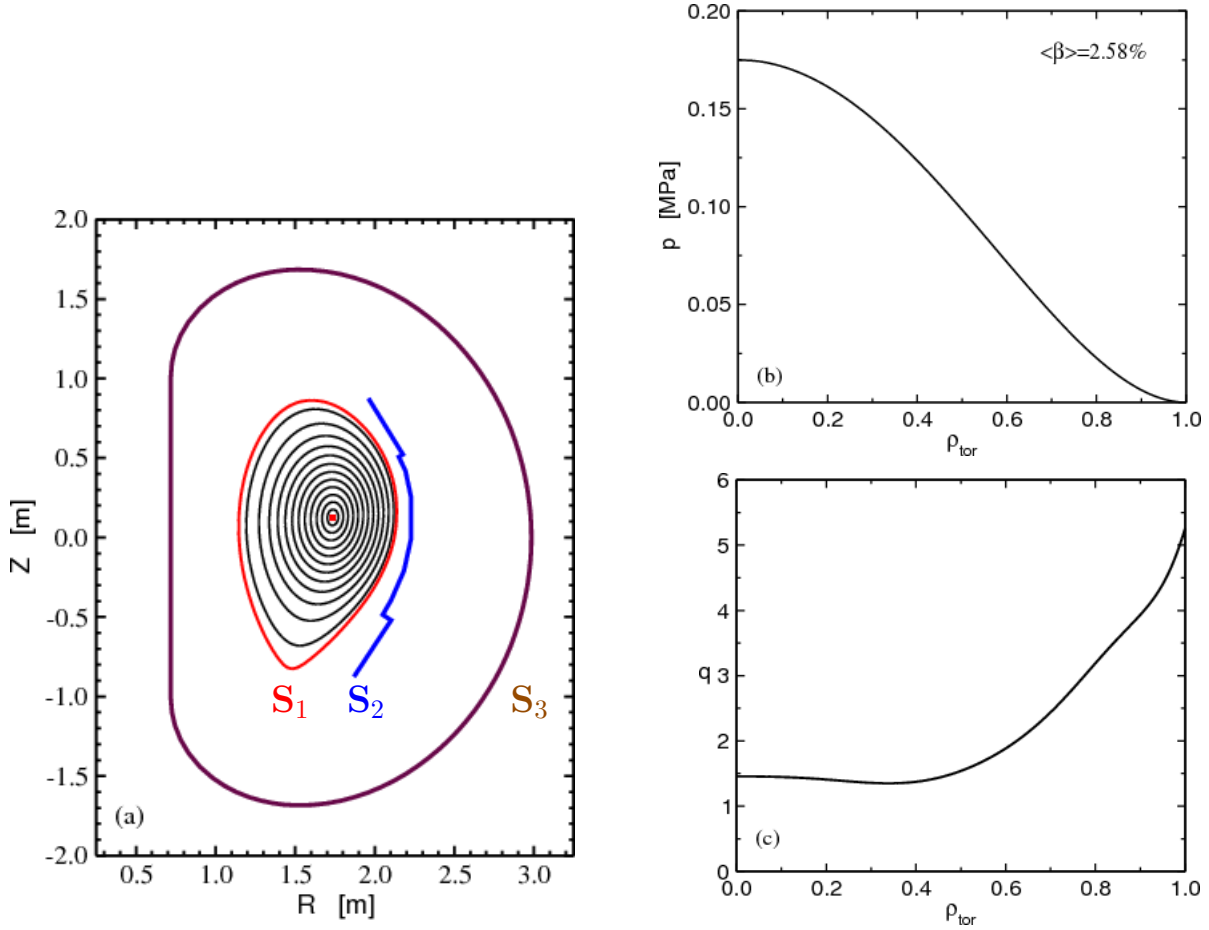


**Fig. 1:** (a) Poloidal cross-section of flux surfaces, plasma boundary ( $S_1$ ), resistive wall ( $S_2$ ), and toroidal field coil ( $S_3$ ), (b) pressure profile, and (c)  $q$ -profile of the ASDEX Upgrade-type test equilibrium ( $\rho_{tor} = \sqrt{s}$ ).

Figure 2a shows a 3D view of the preliminary wall design of ASDEX Upgrade [26]. In Fig. 2b the whole configuration composed of plasma, resistive wall, and 16 toroidal field coils is presented. The latter are modeled by infinitely thin bands of finite width.

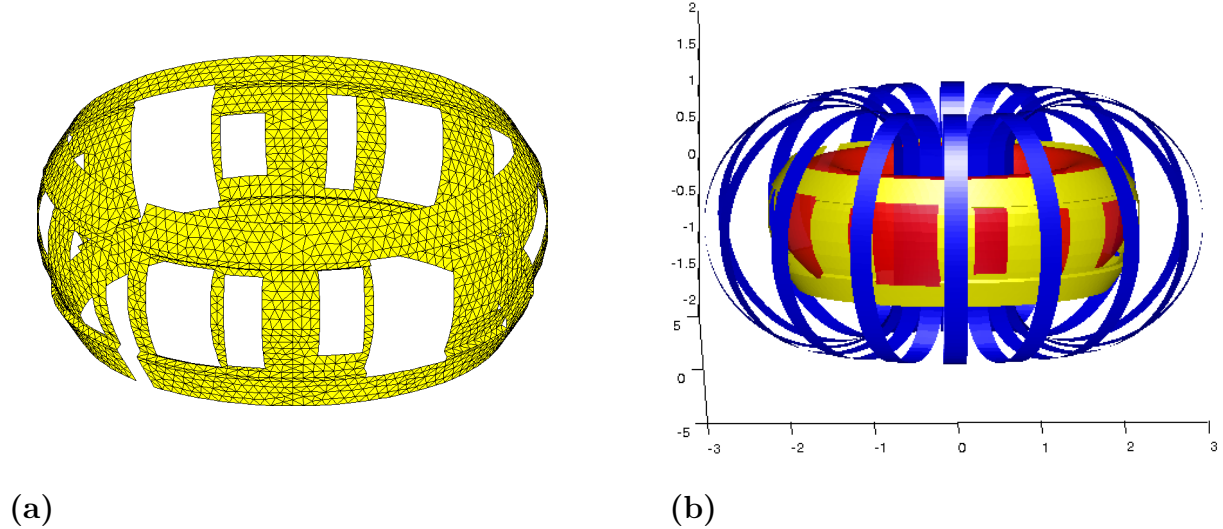


**Fig. 2:** (a) Preliminary design of the resistive wall, and (b) plasma with resistive wall and toroidal field coils.

Without wall the equilibrium is unstable with respect to  $n = 0, 1$  and  $2$  modes ( $n > 2$  are not considered). However, it can be stabilized with an ideal conducting wall sufficiently close to the plasma (see Fig.1a)

In case of a finite wall conductivity the plasma is unstable on a resistive time scale. A surface conductivity  $\sigma d = 2.8 \cdot 10^5$  S was used with  $\sigma$  being the specific conductivity and  $d$  the thickness of the wall.

In Fig. 3a the eigenvalue  $\gamma$  of the  $n = 0$  mode is plotted versus the plasma-wall distance  $r_{shift}$ . The eigenvalue is computed with the CAS3D code including the perturbed kinetic energy term. The  $m = 0, n = 0$  harmonic causes a current in the toroidal field coils producing a net-toroidal field in the region between the plasma boundary and the coils. In Fig. 4 the  $m$ -harmonics of the  $n = 0$  eigenfunction are plotted for the no-wall limit case ( $\gamma = 510481$  1/s). There, the  $m = 0$  harmonic only makes a very small contribution.

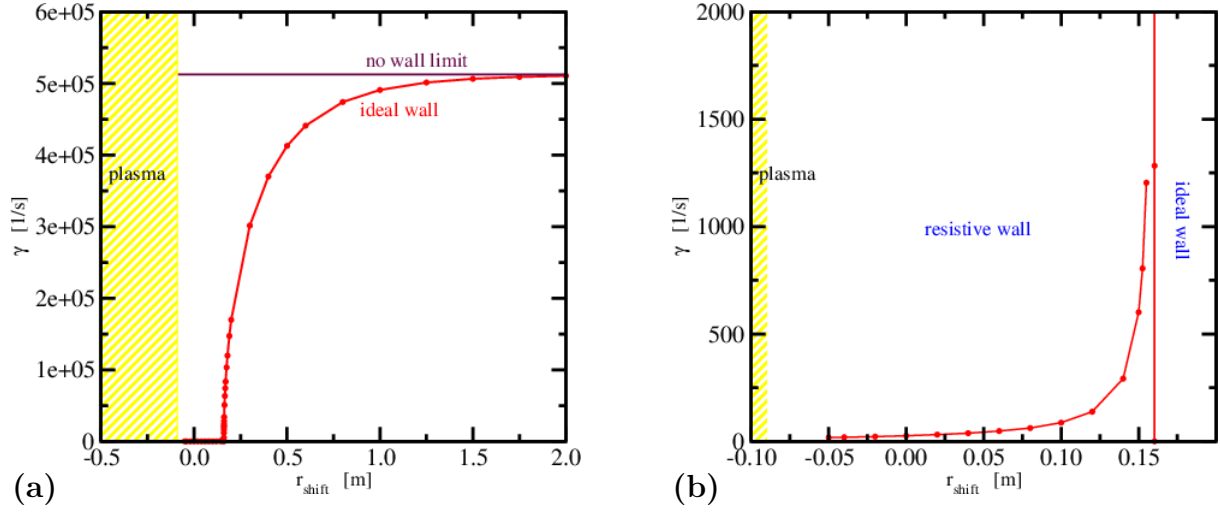


**Fig. 3:** Growth rate of the  $n=0$  mode in dependence of the wall position. The latter is presented by the radial shift of the wall with  $r_{shift} = 0$  being the planned position of the wall in ASDEX Upgrade. The hatched area marks the plasma with its boundary lying approximately 9 cm inside the unshifted wall. The plots show the growth rates assuming an ideal, and a resistive wall, respectively. The plot on the right-hand side presents an enlargement of the left-hand side plot, showing the resistive wall growth rates and the stabilizing ideal wall position at  $r_{shift} = 0.16$  m in detail.

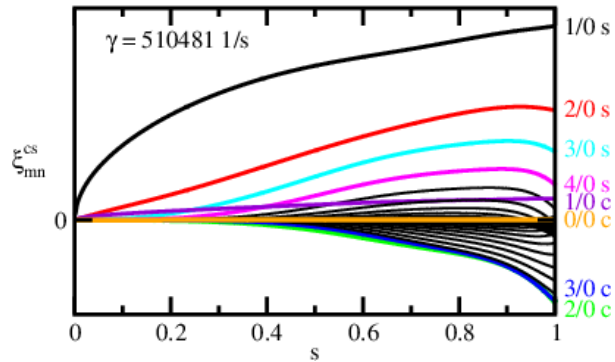


**Fig. 4:** Eigenfunction of the  $n = 0$  mode represented by the cosine and sine Fourier harmonics,  $\xi_{mn}^c, \xi_{mn}^s$ , of the normal component of the displacement vector  $\xi$  as function of  $s$ . Here and in the following plots, the largest harmonics are marked by their poloidal and toroidal indices,  $m/n$ . The  $s$  and  $c$  attached to these numbers characterize the sine and cosine harmonics, respectively. In this plot, additionally, the  $m=0, n=0$  harmonic is marked by the orange line.



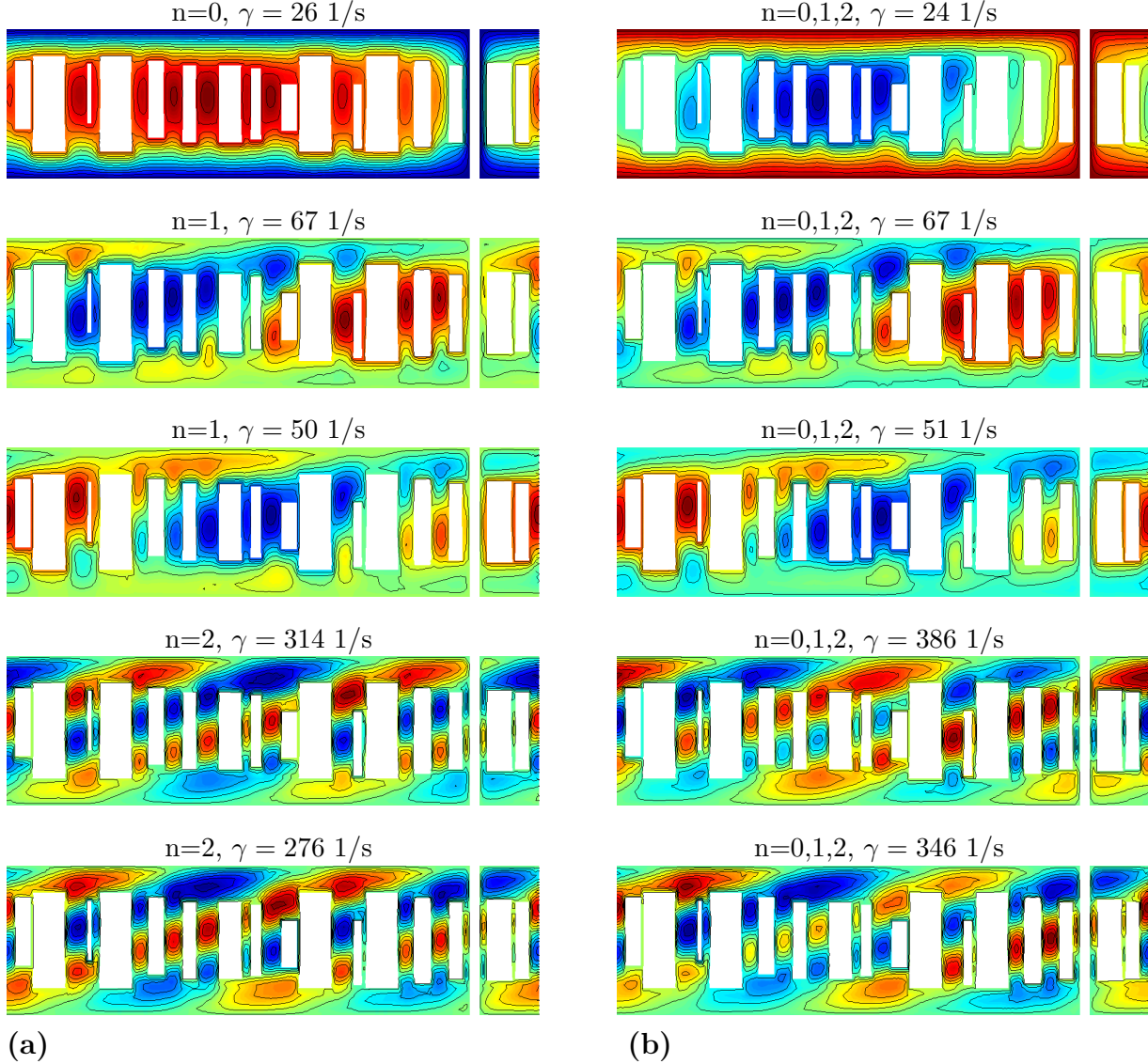


**Fig. 5:** Resistive wall surface currents belonging to the 5 unstable ( $n = 0, 1, 2$ ) multi-mode eigenvalues (b) and to the unstable single  $n = 0, n = 1, n = 2$  eigenvalues (a) are shown. The current pattern of the multi-mode cases can be uniquely related to the single  $n$  solutions.

The axisymmetry is broken by the multiply-connected ASDEX Upgrade resistive wall so that, in principle, all  $n$ -harmonics contribute to an eigenmode. In Fig. 5b surface-current lines of the induced wall currents are shown for the 5 unstable eigenmodes where  $n = 0, 1, 2$  toroidal harmonics have been taken into account. For comparison, in Fig. 5a surface current are shown obtained from single  $n = 0, n = 1$  and  $n = 2$  toroidal mode computation. Comparing the eigenvalues - also quoted in Figs 5a-b - one can uniquely relate the single  $n$  modes to the  $n = 0, 1, 2$  eigenmodes. That is, each eigenmode is

dominated by one  $n$ -harmonic. The asymmetry of the wall geometry leads to a significant splitting of the eigenvalues and coupling of the toroidal harmonics. In Figs 6a-b the two orthogonal eigenfunctions for the ( $n = 2$ ) case with different eigenvalues (see Fig. 5a row 4 and 5) are shown. In order to get a sufficiently good resolution in the neighbourhood of rational surfaces a non-equidistant radial grid has been implemented in the CAS3D code. Figure 7a shows the coupling of the toroidal  $n = 1, n = 2$  harmonics. In Fig. 7b the enlargement of the 3/2-harmonic region demonstrates the improved resolution obtained by the accumulated mesh at the  $q = 3/2$  surface.

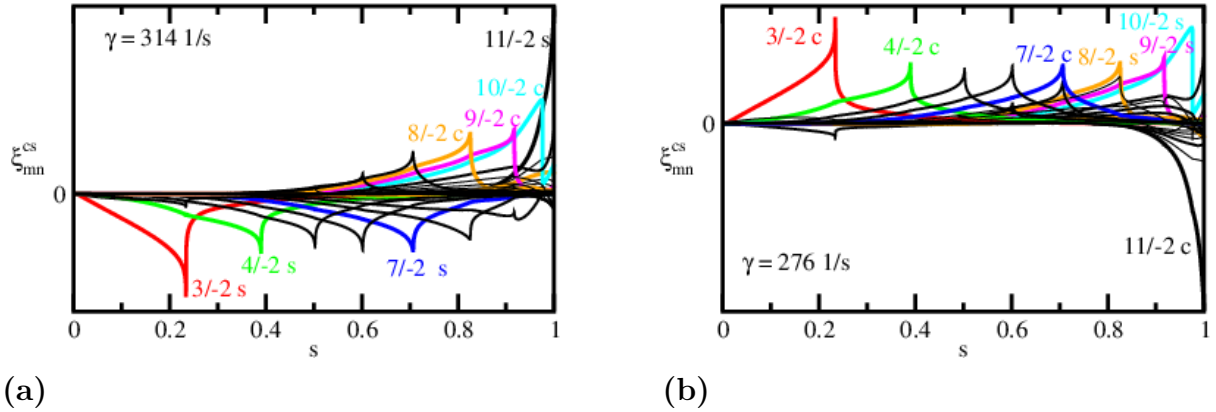


**Fig. 6:** Eigenfunctions of the  $n = 2$  mode in presence of a resistive wall and ideal toroidal field coils. The two plots show the eigenfunction spectra for the two eigenvalues which correspond to the two existing orthogonal solutions.

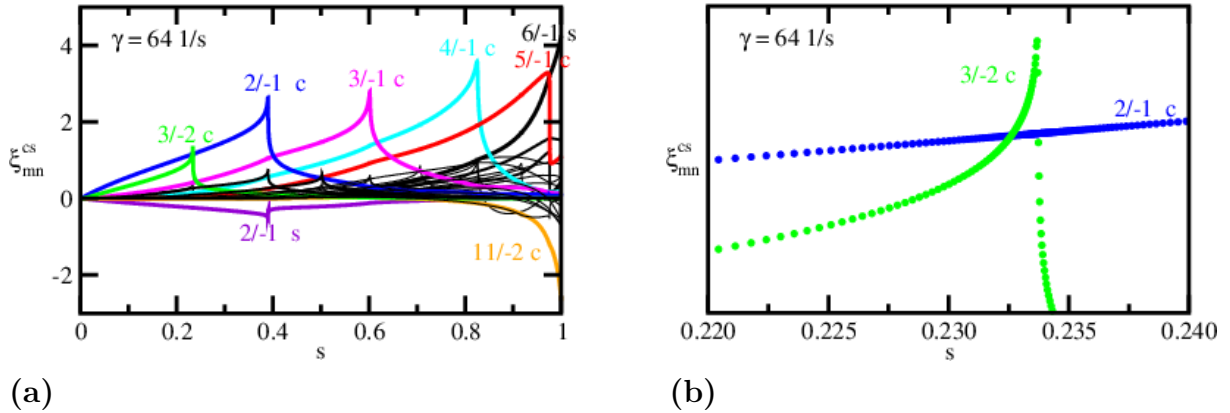


**Fig. 7:** (a) Eigenfunctions of the coupled  $n = 1, n = 2$  mode. (b) Enlargement of the 3/2-harmonic showing the radial grid accumulation around the rational  $q = 3/2$  surface. To obtain the same grid refinement with an equidistant grid 40000 grid points would be necessary compared to 931 non-equidistant grid points.

## 6 Outlook

The STARWALL code is a very flexible numerical tool which can be combined with linear and nonlinear stability codes. The non-linear MHD code JOREK and the linear MHD code CASTOR3D are currently under development using STARWALL for the resistive wall part.

The JOREK-STARWALL code has already been applied to nonlinear studies of resistive wall modes [27], vertical displacement events [28], disruptions triggered by massive gas injection [29] and QH-Mode [30]. Besides a current optimization and parallelization of STARWALL for resolving larger problem sizes, an extension of JOREK-STARWALL to include Halo currents is currently under development [28].

Furthermore, the STARWALL code is used in combination with the CASTOR\_3DW code for stability studies of axisymmetric equilibria in presence of ideal wall structures, including physical effects such as plasma resistivity, viscosity, poloidal and toroidal rotation [31]. Currently, CASTOR3D is under development [14], a hybrid of the CASTOR\_3DW and the STARWALL codes. Solving an extended eigenvalue problem (MHD equations of CASTOR\_3DW and vacuum part of STARWALL), this code takes plasma inertia and resistive walls simultaneously into account. Besides the straight field line coordinates used for the plasma part so far, general flux coordinates are implemented such that linear studies of resistive and rotating 3D equilibria in presence of 3D resistive walls will be possible.

## Acknowledgments

We would like to thank Sibylle Günter, Karl Lackner, and Matthias Hölzl for useful discussions and comments.

## References

- [1] Chu M S and Okabayashi M 2010 ‘Stabilization of the external kink and resistive wall mode.’ *Plasma Phys. Control. Fusion* **52** 123001. doi:10.1088/0741-3335/52/12/123001.
- [2] Bialek J, Boozer A H, Mauel M E, and Navratil G A 2001 ‘Modeling of active control of external magnetohydrodynamic instabilities.’ *Phys. Plasmas* **8**(5) 2170–2180.

- [3] Katsuro-Hopkins O, Bialek J, Maurer D A, and Navratil G A 2007 ‘Enhanced ITER resistive wall mode feedback performance using optimal control techniques.’ *Nucl. Fusion* **47** 1157–1165.
- [4] Chu M, Chance M, Glasser A, and Okabayashi M 2003 ‘Normal mode approach to modelling of feedback stabilization of the resistive wall mode.’ *Nucl. Fusion* **43** 441–454.
- [5] Liu Y, Bondeson A, Gregoratto D, *et al.* 2004 ‘Feedback control of resistive wall modes in toroidal devices.’ *Nucl. Fusion* **44** 77–86.
- [6] Portone A, Villone F, Liu Y, Albanese R, and Rubinacci G 2008 ‘Linearly perturbed MHD equilibria and 3D eddy current coupling via control surface method.’ *Plasma Phys. Control. Fusion* **50** 085004. doi:10.1088/0741-3335/50/8/085004.
- [7] Hirshman S P and Whitson J C 1983 ‘Steepest-descent moment method for three-dimensional magnetohydrodynamic equilibria.’ *Phys. Fluids* **26** 3553.
- [8] Hirshman S P and Lee D K 1986 ‘Momcon: A spectral code for obtaining three-dimensional magnetohydrodynamic equilibria.’ *Comput. Phys. Commun.* **39** 161.
- [9] Hirshman S P, van Rij W I, and Merkel P 1986 ‘Three-dimensional free boundary calculations using a spectral Green’s function method.’ *Comput. Phys. Comm.* **43** 143.
- [10] Nührenberg C 1996 ‘Global ideal magnetohydrodynamic stability analysis for the configurational space of Wendelstein 7-X.’ *Phys. Plasmas* **3** 2401.
- [11] Sempf M, Merkel P, Strumberger E, Tichmann C, and Günter S 2009 ‘Robust control of resistive wall modes using pseudospectra.’ *New J. Phys.* **11** 053015. doi:10.1088/1367-2630/11/5/053015.
- [12] Hölzl M, Merkel P, Huysmans G, *et al.* 2012 ‘Coupling JOEK and STARWALL codes for non-linear resistive-wall simulations.’ *Journal of Physics: Conference Series* **401** 012010. doi:10.1088/1742-6596/401/1/012010.
- [13] Huysmans G T A and Czarny O 2007 ‘MHD stability in X-point geometry: simulation of ELMS.’ *Nucl. Fusion* **47** 659. doi:10.1088/0029-5515/47/7/016.
- [14] Strumberger E, Günter S, Merkel P, and Tichmann C 2014 ‘Linear stability studies including resistive wall effects with the CASTOR/STARWALL code.’ *Journal of Physics: Conference Series* **561** 012016. doi:10.1088/1742-6596/561/1/012016.

- [15] Merkel P, Nührenberg C, and Strumberger E 2004 ‘Resistive wall modes of 3D equilibria with multiply-connected walls.’ In *31st EPS Conf. on Contr. Fusion and Plasma Phys.*. ECA Vol. 28G P-1.208, London, UK.
- [16] Merkel P and Sempf M 2006 ‘Feedback stabilization of resistive wall modes in the presence of multiply-connected wall structures.’ In *Fusion Energy 2006*. (Proc. 21st Int. Conf., Chengdu, 2006) (Vienna: IAEA), CD-ROM file TH/P3-8, and <http://www-naweb.iaea.org/naweb/physics/FEC/FEC2006/html/index.htm>.
- [17] Günter S, Lauber P, Merkel M, *et al.* 2008 ‘Three-dimensional effects in tokamaks.’ *Plasma Phys. Control. Fusion* **50** 124004. doi:10.1088/0741-3335/50/12/124004.
- [18] Strumberger E, Merkel P, Sempf M, and Günter S 2008 ‘On fully three-dimensional resistive wall mode and feedback stabilization computations.’ *Phys. Plasmas* **15** 056110. doi:10.1063/1.2884579.
- [19] Kallenbach A, Bobkov V, Braun F, *et al.* 2011 ‘ASDEX Upgrade results and future plans.’ In *38th IEEE International Conference on Plasma Science (ICOPS) and 24th Symposium on Fusion Engineering (SOFE)*. SPL5-1, Chicago, IL.
- [20] Lüst R and Martensen E 1960 ‘Zur Mehrwertigkeit des skalaren magnetischen Potentials beim hydromagnetischen Stabilitätsproblem eines Plasmas.’ *Z. Naturforschung* **15a** 706.
- [21] Merkel P 1986 ‘An integral equation technique for the exterior and interior Neumann problem in toroidal regions.’ *J. Comput. Physics* **66** 83.
- [22] Merkel P 1988 ‘Applications of the Neumann problem to stellarators: magnetic surfaces, coils, free-boundary equilibrium, magnetic diagnostic.’ *Theory of Fusion Plasmas Varenna 1987, EUR 11336 EN* 25.
- [23] Haney S W and Freidberg J P 1989 ‘Variational methods for studying tokamak stability in the presence of a thin wall.’ *Phys. Fluids B* **1** 1637.
- [24] Bernstein I B, Frieman E A, Kruskal M D, and Kulsrud R M 1958 ‘An energy principle for hydromagnetic stability problems.’ *Proc. R. Soc. Lond.* **244** 17–40.
- [25] Nührenberg J and Zille R 1988 ‘Equilibrium and stability of low-shear stellarators.’ *Theory of Fusion Plasmas Varenna 1987, EUR 11336 EN* 3.

- [26] Suttrop W, Gruber O, Günter S, *et al.* 2009 ‘In-vessel saddle coils for MHD control in ASDEX Upgrade.’ *Fusion Engineering and Design* **84** 290. doi:10.1016/j.fusengdes.2008.12.044.
- [27] McAdams R 2014 *Non-linear Magnetohydrodynamic Instabilities in Advanced Tokamak Plasmas*. Ph.D. thesis, University of York.
- [28] Hölzl M, Huysmans G, Merkel P, *et al.* 2014 ‘Non-linear simulations of MHD instabilities in tokamaks including eddy current effects and perspectives for the extension to halo currents.’ *Journal of Physics: Conference Series* **561** 012011.
- [29] Fil A, Nardon E, Hoelzl M, *et al.* 2015 ‘Modeling a massive gas injection triggered disruption in JET with the JOREK code.’ *Physics of Plasmas* **22** 062509.
- [30] Liu F, Huijsmans G, Loarte A, *et al.* 2014 ‘Nonlinear MHD simulations of QH-mode plasmas in DIII-D.’ In *Proceedings of the 41st EPS Conference on Plasma Physics*. Berlin, Germany. O5.135.
- [31] Strumberger E, Merkel P, Tichmann C, and Günter S 2011 ‘Linear stability studies in the presence of 3D wall structures.’ In *38th EPS Conf. on Plasma Phys.* ECA Vol. 35G P5.082, Strasbourg, France.
- [32] Wimp J 1984 ‘Computation with recurrence relations.’ *Pitman Publishing Inc., London* 305.
- [33] Wong R 1989 ‘Asymptotic approximation of integrals.’ *Academic Press. Inc, San Diego* 432.

## 7 Appendix

### A Lagrangians

The variational method will be explained by starting with a simple problem. For a current  $\mathbf{j}$  on an ideal conducting torus one can define the following variational problem: determine the current distribution by minimizing the energy of the magnetic field produced. The Lagrangian - being the magnetic energy - is given by

$$\mathcal{L}_S = \frac{1}{8\pi} \int_S df \int_S df' \frac{\mathbf{j} \cdot \mathbf{j}'}{|\mathbf{r} - \mathbf{r}'|} \quad (\text{A.1})$$

with the divergence-free surface current

$$\mathbf{j} = \mathbf{n} \times \nabla \Phi, \quad \Phi = I^P v + I^T u + \phi(u, v) \quad (\text{A.2})$$

with angle-like surface coordinates  $u, v : 0 \leq u \leq 1, 0 \leq v \leq 1$ .

Given a net-poloidal current  $I^P$  and/or a net-toroidal current  $I^T$  one gets the "Euler equation" by varying  $\mathcal{L}_S$  with respect to the single-valued potential  $\phi(u, v)$ .

$$\delta \mathcal{L}_S = \frac{1}{4\pi} \int_S df \int_S df' \frac{\delta \mathbf{j} \cdot \mathbf{j}'}{|\mathbf{r} - \mathbf{r}'|} = \int_S df \delta \mathbf{j} \cdot \mathbf{A} \quad (\text{A.3})$$

and with

$$\delta \mathbf{j} = \frac{\mathbf{r}_u \frac{\partial}{\partial v} \delta \phi - \mathbf{r}_v \frac{\partial}{\partial u} \delta \phi}{|\mathbf{r}_v \times \mathbf{r}_u|} \quad (\text{A.4})$$

$$\begin{aligned} \delta \mathcal{L}_S &= \int_S du dv (\mathbf{r}_u \frac{\partial}{\partial v} \delta \phi - \mathbf{r}_v \frac{\partial}{\partial u} \delta \phi) \cdot \mathbf{A} = - \int_S du dv \delta \phi (\mathbf{r}_u \frac{\partial}{\partial v} - \mathbf{r}_v \frac{\partial}{\partial u}) \cdot \mathbf{A} \\ &= - \int_S du dv \delta \phi [\mathbf{r}_u (\mathbf{r}_v \cdot \nabla) - \mathbf{r}_v (\mathbf{r}_u \cdot \nabla)] \cdot \mathbf{A} \\ &= - \int_S du dv \delta \phi (\mathbf{r}_v \times \mathbf{r}_u) \cdot (\nabla \times \mathbf{A}) = - \int_S du dv \delta \phi (\mathbf{r}_v \times \mathbf{r}_u) \cdot \mathbf{B} \end{aligned} \quad (\text{A.5})$$

From  $\delta \mathcal{L}_S = 0$  it follows the so-called natural boundary condition  $\mathbf{n} \cdot \mathbf{B} = 0$ .

There are two independent solutions. Given a net-poloidal current  $I^P$  the magnetic field  $\mathbf{B}$  vanishes in the exterior region of the toroidal surface and given a net-toroidal current  $I^T$  the field  $\mathbf{B}$  vanishes in the interior region. For the problem considered one got the natural

boundary condition  $\mathbf{n} \cdot \mathbf{B} = 0$ . In order to obtain more general boundary conditions one has to add appropriate terms. One gets the Lagrangian  $\mathcal{L}_V$  for the configuration treated in section 3 by terms of type (A.1) and adding a term linear in  $\mathbf{j}$  appropriate to satisfy the boundary condition at the plasma-vacuum interface  $S_1$  and a term to fulfil the boundary condition at the resistive wall  $S_2$ .

$$\mathcal{L}_V = \frac{1}{8\pi} \sum_{i=1}^3 \sum_{k=1}^3 \int_{S_i} df_i \int_{S_k} df_k \frac{\mathbf{j}_i \cdot \mathbf{j}_k}{|\mathbf{r}_i - \mathbf{r}_k|} + \frac{1}{2\gamma} \int_{S_2} df_2 \frac{\mathbf{j}_2 \cdot \mathbf{j}_2}{\sigma d} + \int_{S_1} df_1 (\mathbf{n}_1 \cdot \boldsymbol{\xi}) \mathbf{n}_1 \cdot (\mathbf{j}_1 \times \mathbf{B}_0) \quad (\text{A.6})$$

To study feedback stabilisation one has to extend the Lagrangian by adding terms for sensor and feedback coils and for feedback voltages given by

$$\begin{aligned} \mathcal{L}_S &= \frac{1}{8\pi} \sum_{l,l'=1}^{n_c, n_c} I_l^c I_{l'}^c \int_{C_l} df_l \int_{C_{l'}} df_{l'} \frac{\mathbf{v}_l \cdot \mathbf{v}_{l'}}{|\mathbf{r}_l - \mathbf{r}_{l'}|} + \frac{1}{4\pi} \sum_l^{n_c} I_l^c \int_{C_l} df_l \sum_{i=1}^3 \int_{S_i} df_i \frac{\mathbf{j}_i \cdot \mathbf{v}_l}{|\mathbf{r}_i - \mathbf{r}_l|} \\ &+ \frac{1}{2\gamma} \sum_{l=1}^{n_c} R_l I_l^c \int_{C_l} df_l \mathbf{v}_l^2 + \frac{1}{\gamma} \sum_{l=1}^{n_c} I_l^c U_{c,l}^{feedb}. \end{aligned} \quad (\text{A.7})$$

with  $n_c$  = number of coils,  $I_\ell^c$  = coil currents,  $R_\ell$  = coil resistance and feedback voltages  $U_{c,\ell}^{feedb}$ .

Considering the variation of the Lagrangian  $\mathcal{L}_V$  (A.6) with respect to  $\Phi_i$ ,  $i = 1, 2, 3$  gives

$$\begin{aligned} \delta \mathcal{L}_V &= \sum_{i=1}^3 \left( \delta I_i^P \int_{S_i} du dv \mathbf{r}_{i,u} \cdot \mathbf{A} - \delta I_i^T \int_{S_i} du dv \mathbf{r}_{i,v} \cdot \mathbf{A} - \int_{S_i} du dv \delta \phi_i (\mathbf{r}_{i,v} \times \mathbf{r}_{i,u}) \cdot \mathbf{B} \right) \\ &- (F_T' \delta I_1^P + F_P' \delta I_1^T) \int_{S_1} du dv \nabla s \cdot \boldsymbol{\xi} + \int_{S_1} du dv \delta \phi_1 \left( F_T' \frac{\partial}{\partial v} + F_P' \frac{\partial}{\partial u} \right) \nabla s \cdot \boldsymbol{\xi} \quad (\text{A.8}) \\ &+ \delta I_2^P \int_{S_2} du dv \frac{\mathbf{r}_{2,u} \cdot \mathbf{j}_2}{\gamma \sigma d} - \delta I_2^T \int_{S_2} du dv \frac{\mathbf{r}_{2,v} \cdot \mathbf{j}_2}{\gamma \sigma d} - \int_{S_2} du dv \delta \phi_2 \frac{\mathbf{r}_{2,v} \cdot \mathbf{j}_{2,u} - \mathbf{r}_{2,u} \cdot \mathbf{j}_{2,v}}{\gamma \sigma d} \end{aligned}$$

with

$$\mathbf{A}(\mathbf{r}) = \frac{1}{4\pi} \sum_{k=1}^3 \int_{S_k} df_k \frac{\mathbf{j}_k}{|\mathbf{r} - \mathbf{r}_k|} \quad (\text{A.9})$$



From  $\delta\mathcal{L}_V = 0$  one gets the boundary conditions at the plasma-vacuum interface  $S_1$

$$\begin{aligned} \int_{S_1} du dv \mathbf{r}_{1,u} \cdot \mathbf{A}(\mathbf{r}_1) &= F'_T \int_{S_1} du dv (\nabla s \cdot \boldsymbol{\xi}), \\ \int_{S_1} du dv \mathbf{r}_{1,v} \cdot \mathbf{A}(\mathbf{r}_1) &= -F'_P \int_{S_1} du dv (\nabla s \cdot \boldsymbol{\xi}) \\ (\mathbf{r}_{1,v} \times \mathbf{r}_{1,u}) \cdot \mathbf{B}(\mathbf{r}_1) &= (F'_T \frac{\partial}{\partial v} + F'_P \frac{\partial}{\partial u})(\nabla s \cdot \boldsymbol{\xi}) \end{aligned} \quad (\text{A.10})$$

at the resistive wall  $S_2$

$$\begin{aligned} \int_{S_2} du dv \mathbf{r}_{2,u} \cdot \mathbf{A}(\mathbf{r}_2) &= \int_{S_2} du dv \frac{\mathbf{r}_{2,u} \cdot \mathbf{j}_2}{\gamma \sigma d} \\ \int_{S_2} du dv \mathbf{r}_{2,v} \cdot \mathbf{A}(\mathbf{r}_2) &= \int_{S_2} du dv \frac{\mathbf{r}_{2,v} \cdot \mathbf{j}_2}{\gamma \sigma d} \\ (\mathbf{r}_{2,v} \times \mathbf{r}_{2,u}) \cdot \mathbf{B}(\mathbf{r}_2) &= \frac{\mathbf{r}_{2,v} \cdot \mathbf{j}_{2,u} - \mathbf{r}_{2,u} \cdot \mathbf{j}_{2,v}}{\gamma \sigma d} \end{aligned} \quad (\text{A.11})$$

and at the external ideal wall  $S_3$

$$\int_{S_3} du dv \mathbf{r}_{3,u} \cdot \mathbf{A}(\mathbf{r}_3) = 0, \quad \int_{S_3} du dv \mathbf{r}_{3,v} \cdot \mathbf{A}(\mathbf{r}_3) = 0, \quad (\mathbf{r}_{3,v} \times \mathbf{r}_{3,u}) \cdot \mathbf{B}(\mathbf{r}_3) = 0 \quad (\text{A.12})$$

The boundary conditions (A.10,A.11,A.12) obtained for  $\mathbf{A}$  are integrals. With an appropriate gauge  $\mathbf{A} \rightarrow \mathbf{A} + \nabla\Psi$  one can get the local conditions (7).

As shown before, on a toroidal surface there exists for an arbitrary prescribed net-poloidal(net-toroidal) current  $I^P$  ( $I^T$ ) a so-called 'equilibrium' current distribution  $\mathbf{j}_{eq}^P$  ( $\mathbf{j}_{eq}^T$ ) generating a magnetic field with vanishing normal component on the surface. The field produced by such a poloidal current on  $S_1$  and a toroidal current on  $S_3$  is zero in the domain bounded by the boundaries  $S_1$  and  $S_3$ . With these equilibrium currents one can compensate the  $I_1^P$  and  $I_3^T$  contributions to the solution. Therefore one can omit these terms.

## B Inductance matrices

The elements of the matrices  $\mathbf{M}_{ij}$ ,  $i, j = 1, 2, 3$  in (17)

$$\mathbf{M}_{ij} = \begin{pmatrix} g_{11}^{ij} & g_{12}^{ij} & g_{1c'}^{ij} & -g_{1s'}^{ij} \\ g_{21}^{ij} & g_{22}^{ij} & g_{2c'}^{ij} & -g_{2s'}^{ij} \\ g_{c1}^{ij} & g_{c2}^{ij} & g_{cc'}^{ij} & -g_{cs'}^{ij} \\ -g_{s1}^{ij} & -g_{s2}^{ij} & -g_{sc'}^{ij} & g_{ss'}^{ij} \end{pmatrix} \quad (\text{B.1})$$

are defined by

$$\begin{aligned}
g_{cc'}^{ij}(k, k') &= \frac{1}{4\pi} \int_{S_i} dx \int_{S_j} dx' \cos(kx) \frac{(k\mathbf{R}_{i,x}) \cdot (k'\mathbf{R}_{j,x'})}{|\mathbf{r}_i - \mathbf{r}'_j|} \cos(k'x') \\
g_{1c'}^{ij}(k') &= -\frac{1}{4\pi} \int_{S_i} dx \int_{S_j} dx' \frac{\mathbf{r}_{i,v} \cdot (k'\mathbf{R}_{j,x'})}{|\mathbf{r}_i - \mathbf{r}'_j|} \cos(k'x') \\
g_{2c'}^{ij}(k') &= \frac{1}{4\pi} \int_{S_i} dx \int_{S_j} dx' \frac{\mathbf{r}_{i,u} \cdot (k'\mathbf{R}_{j,x'})}{|\mathbf{r}_i - \mathbf{r}'_j|} \cos(k'x') \\
g_{11}^{ij} &= \frac{1}{4\pi} \int_{S_i} dx \int_{S_j} dx' \frac{\mathbf{r}_{i,v} \cdot \mathbf{r}_{j,v'}}{|\mathbf{r}_i - \mathbf{r}'_j|}, \quad g_{12}^{ij} = -\frac{1}{4\pi} \int_{S_i} dx \int_{S_j} dx' \frac{\mathbf{r}_{i,v} \cdot \mathbf{r}_{j,u'}}{|\mathbf{r}_i - \mathbf{r}'_j|} \\
g_{21}^{ij} &= -\frac{1}{4\pi} \int_{S_i} dx \int_{S_j} dx' \frac{\mathbf{r}_{i,u} \cdot \mathbf{r}_{j,v'}}{|\mathbf{r}_i - \mathbf{r}'_j|}, \quad g_{22}^{ij} = \frac{1}{4\pi} \int_{S_i} dx \int_{S_j} dx' \frac{\mathbf{r}_{i,u} \cdot \mathbf{r}_{j,u'}}{|\mathbf{r}_i - \mathbf{r}'_j|}
\end{aligned} \tag{B.2}$$

with the notation

$$k = 2\pi(m, n), \quad x = (u, v)^\top, \quad dx = du \, dv, \quad \mathbf{R}_{i,x} = (-\mathbf{r}_{i,v}, \mathbf{r}_{i,u})^\top, \quad F = (F'_P, F'_T)^\top \tag{B.3}$$

The matrix elements with sine are defined accordingly.

The elements of matrix  $\mathbf{N}_{22}$  in (17)

$$\mathbf{N}_{22} = \begin{pmatrix} h_{11} & h_{12} & h_{1c'} & -h_{1s'} \\ h_{21} & h_{22} & h_{2c'} & -h_{2s'} \\ h_{c1} & h_{c2} & h_{cc'} & -h_{cs'} \\ -h_{s1} & -h_{s2} & -h_{sc'} & h_{ss'} \end{pmatrix} \tag{B.4}$$

are defined as

$$\begin{aligned}
h_{cc'}(k, k') &= \frac{1}{4\pi^2} \int_{S_2} dx \frac{(k\mathbf{R}_{2,x}) \cdot (k'\mathbf{R}_{2,x})}{|\mathbf{r}_{2,v} \times \mathbf{r}_{2,u}|} \cos(kx) \cos(k'x) \\
h_{1c'}(k') &= \frac{1}{2\pi} \int_{S_2} dx \frac{\mathbf{r}_{2,v} \cdot (k'\mathbf{R}_{2,x'})}{|\mathbf{r}_{2,v} \times \mathbf{r}_{2,u}|} \cos(k'x) \\
h_{2c'}(k') &= \frac{1}{2\pi} \int_{S_2} dx \frac{\mathbf{r}_{2,u} \cdot (k'\mathbf{R}_{2,x'})}{|\mathbf{r}_{2,v} \times \mathbf{r}_{2,u}|} \cos(k'x) \\
h_{11} &= \int_{S_2} dx \frac{\mathbf{r}_{2,v} \cdot \mathbf{r}_{2,v}}{|\mathbf{r}_{2,v} \times \mathbf{r}_{2,u}|}, \quad h_{12} = \int_{S_2} dx \frac{\mathbf{r}_{2,v} \cdot \mathbf{r}_{2,u}}{|\mathbf{r}_{2,v} \times \mathbf{r}_{2,u}|} \\
h_{21} &= \int_{S_2} dx \frac{\mathbf{r}_{2,u} \cdot \mathbf{r}_{2,v}}{|\mathbf{r}_{2,v} \times \mathbf{r}_{2,u}|}, \quad h_{22} = \int_{S_2} dx \frac{\mathbf{r}_{2,u} \cdot \mathbf{r}_{2,u}}{|\mathbf{r}_{2,v} \times \mathbf{r}_{2,u}|}
\end{aligned} \tag{B.5}$$

and the matrix elements with sine are defined accordingly.

The matrix  $\mathbf{M}_{1\xi}$  (17) is defined by <sup>1</sup>

$$\mathbf{M}_{1\xi} = \left( \begin{array}{ccc|ccc} 0 & 0 & 0 & -F'_P & 0 & 0 & 0 \\ 0 & 0 & 0 & -F'_T & 0 & 0 & 0 \\ \hline 0 & 0 & 0 & 0 & \ddots & 0 & 0 \\ 0 & 0 & 0 & 0 & 0 & -\frac{1}{2}kF\delta_{k,k'} & 0 \\ 0 & 0 & 0 & 0 & 0 & 0 & \ddots \\ \hline \ddots & 0 & 0 & 0 & 0 & 0 & 0 \\ 0 & \frac{1}{2}kF\delta_{k,k'} & 0 & 0 & 0 & 0 & 0 \\ 0 & 0 & \ddots & 0 & 0 & 0 & 0 \end{array} \right) \quad (\text{B.6})$$

The matrices  $\mathbf{M}_{\xi i}$ ,  $i = 1, 2, 3$  in (26) are obtained by discretizing the vacuum energy term

$$\mathbf{M}_{\xi i} = \begin{pmatrix} b_{s1}^i & b_{s2}^i & b_{ss'}^i & b_{sc'}^i \\ \delta_{1,i}F'_P & (\delta_{1,i} - 1)F'_T & 0 & 0 \\ b_{c1}^i & b_{c2}^i & b_{cs'}^i & b_{cc'}^i \end{pmatrix} \quad (\text{B.7})$$

$$b_{s1}^i(k) = -\frac{1}{4\pi} \int_{S_i} dx \sin(kx) d_1^i(u, v), \quad b_{s2}^i(k) = \frac{1}{4\pi} \int_{S_i} dx \sin(kx) d_2^i(u, v) \quad (\text{B.8})$$

with

$$\begin{aligned} d_1^1(u, v) &= (F'_P \mathbf{r}_{1,u} + F'_T \mathbf{r}_{1,v}) \cdot \int_{S_1} du' dv' \mathbf{r}_{1,v'} \times \frac{(\mathbf{r}_1 - \mathbf{r}'_1)}{|\mathbf{r}_1 - \mathbf{r}'_1|^3} - 2\pi F'_P \\ d_1^i(u, v) &= (F'_P \mathbf{r}_{1,u} + F'_T \mathbf{r}_{1,v}) \cdot \int_{S_i} du' dv' \mathbf{r}_{i,v'} \times \frac{(\mathbf{r}_1 - \mathbf{r}'_i)}{|\mathbf{r}_1 - \mathbf{r}'_i|^3}, \quad i = 2, 3 \\ d_2^1(u, v) &= (F'_P \mathbf{r}_{1,u} + F'_T \mathbf{r}_{1,v}) \cdot \int_{S_1} du' dv' \mathbf{r}_{1,u'} \times \frac{(\mathbf{r}_1 - \mathbf{r}'_1)}{|\mathbf{r}_1 - \mathbf{r}'_1|^3} + 2\pi F'_T \\ d_2^i(u, v) &= (F'_P \mathbf{r}_{1,u} + F'_T \mathbf{r}_{1,v}) \cdot \int_{S_i} du' dv' \mathbf{r}_{i,u'} \times \frac{(\mathbf{r}_1 - \mathbf{r}'_i)}{|\mathbf{r}_1 - \mathbf{r}'_i|^3}, \quad i = 2, 3 \end{aligned} \quad (\text{B.9})$$

and with  $F = (F'_P, F'_T)^\top$

$$\begin{aligned} b_{ss'}^i(k, k') &= -\frac{1}{2}(kF) \int_{S_i} dx \cos(kx) a_{s'}^i(u, v, k') \\ b_{cc'}^i(k, k') &= -\frac{1}{2}(kF) \int_{S_i} dx \sin(kx) a_{c'}^i(u, v, k') \\ b_{sc'}^i(k, k') &= -\frac{1}{2}(kF) \left( \pi \delta_{k,k'} \delta_{1,i} + \int_{S_i} dx \cos(kx) a_{c'}^i(u, v, k') \right) \\ b_{cs'}^i(k, k') &= \frac{1}{2}(kF) \left( \pi \delta_{k,k'} \delta_{1,i} + \int_{S_i} dx \sin(kx) a_{s'}^i(u, v, k') \right) \end{aligned} \quad (\text{B.10})$$

---

<sup>1</sup>note:  $\delta_{k,k'} = \delta_{m,m'} \delta_{n,n'}$

with

$$\begin{aligned}
a_{s'}^1(u, v, k') &= \int_{S_1} dx' (\mathbf{r}_{1,v'} \times \mathbf{r}_{1,u'}) \cdot \frac{(\mathbf{r}_1 - \mathbf{r}'_1)}{|\mathbf{r}_1 - \mathbf{r}'_1|^3} \sin(k'x') \\
a_{s'}^i(u, v, k') &= \int_{S_1} dx' (\mathbf{r}_{1,v'} \times \mathbf{r}_{1,u'}) \cdot \frac{(\mathbf{r}_i - \mathbf{r}'_1)}{|\mathbf{r}_i - \mathbf{r}'_1|^3} \sin(k'x'), \quad i = 2, 3
\end{aligned} \tag{B.11}$$

and  $a_{c'}^i(u, v, k')$  accordingly.

## C The subtraction method

The elements of the self-inductance matrix  $\mathbf{M}_{11}$  (B.1) and (B.2) are Fourier integrals over the plasma-vacuum interface. The integrands are singular so that a standard numerical Fourier transform is not possible. The problem is solved by applying a subtraction method: An analytically integrable function with the same singular behaviour is subtracted. The analytical integral is then added to the numerically Fourier-transformed regularized function.

The subtraction method will be demonstrated by treating a term of (B.2).

$$\hat{g}(m, n; m', n') = \int_0^1 du \int_0^1 dv \int_0^1 du' \int_0^1 dv' g(u, v; u', v') e^{2\pi i(mu+nv-m'u'-n'v')} \tag{C.1}$$

with

$$g(u, v; u', v') = \frac{\mathbf{r}_u \cdot \mathbf{r}_{u'}}{|\mathbf{r}(u, v) - \mathbf{r}(u', v')|} \tag{C.2}$$

Expanding  $g$  at the singularity

$$\mathbf{r}' - \mathbf{r} = \mathbf{r}_u \delta u + \mathbf{r}_v \delta v + \mathbf{r}_{uu} \frac{\delta u^2}{2} + \mathbf{r}_{uv} \delta u \delta v + \mathbf{r}_{vv} \frac{\delta v^2}{2}$$

with  $\delta u = u' - u$ ,  $\delta v = v' - v$  and replacing  $\delta u, \delta v$  by  $\tan(\pi \delta u)/\pi, \tan(\pi \delta v)/\pi$  one gets a periodic function which can be Fourier-transformed analytically with respect to  $u'$  and  $v'$ .

$$\begin{aligned}
&g_{sing}(u, v; u' - u, v' - v) \\
&= \frac{\pi \mathbf{r}_u^2}{\sqrt{\mathbf{r}_u^2 \tan^2(\pi(u'-u)) + 2 \mathbf{r}_u \cdot \mathbf{r}_v \tan(\pi(u'-u)) \tan(\pi(v'-v)) + \mathbf{r}_v^2 \tan^2(\pi(v'-v))}}
\end{aligned} \tag{C.3}$$

With the analytically computable integrals (see appendix D)

$$I(m, n; a, b, c) = \int_0^1 du \int_0^1 dv \frac{\pi e^{2\pi i(mu+nv)}}{\sqrt{a \tan^2(\pi u) + 2 b \tan(\pi u) \tan(\pi v) + c \tan^2(\pi v)}} \quad (\text{C.4})$$

one finds for the singular integral

$$\hat{g}_{sing}(m, n; m', n') = \int_0^1 du \int_0^1 dv \mathbf{r}_u^2 I(m', n'; \mathbf{r}_u^2, \mathbf{r}_u \cdot \mathbf{r}_v, \mathbf{r}_v^2) e^{2\pi i((m-m')u+(n-n')v)} \quad (\text{C.5})$$

The regularized part can be Fourier transformed numerically

$$\begin{aligned} \hat{g}_{reg}(m, n; m', n') &= \quad (\text{C.6}) \\ &= \int_0^1 du \int_0^1 dv \int_0^1 du' \int_0^1 dv' (g(u, v; u', v') - g_{sing}(u, v; u' - u, v' - v)) e^{2\pi i(mu+nv-m'u'-n'v')} \end{aligned}$$

so that the Fourier transform of  $g(u, v; u', v')$  is given by

$$\hat{g}(m, n; m', n') = \hat{g}_{reg}(m, n; m', n') + \hat{g}_{sing}(m, n; m', n') \quad (\text{C.7})$$

A second type of singular integrals appears in a part of the vacuum energy matrix  $\mathbf{M}_{\hat{\xi}_1}$  (B.7) -(B.11). The subtraction method will be demonstrated for a term in (B.11)

$$\hat{h}(u, v; m', n') = \int_0^1 du' \int_0^1 dv' h(u, v; u', v') e^{2\pi i(m'u'+n'v')} \quad (\text{C.8})$$

with

$$h(u, v; u', v') = \frac{(\mathbf{r}_v \times \mathbf{r}_{u'}) \cdot (\mathbf{r}(u, v) - \mathbf{r}(u', v'))}{|\mathbf{r}(u, v) - \mathbf{r}(u', v')|^3} \quad (\text{C.9})$$

the expansion of the integrand at the singularity is given by

$$\begin{aligned} h_{sing}(u, v; u' - u, v' - v) &= \quad (\text{C.10}) \\ \frac{\pi(\mathbf{r}_v \times \mathbf{r}_u)}{2} \cdot \frac{\mathbf{r}_{uu} \tan^2(\pi(u'-u)) + 2 \mathbf{r}_{uv} \tan(\pi(u'-u)) \tan(\pi(v'-v)) + \mathbf{r}_{vv} \tan^2(\pi(v'-v))}{(\mathbf{r}_u^2 \tan^2(\pi(u'-u)) + 2 \mathbf{r}_u \cdot \mathbf{r}_v \tan(\pi(u'-u)) \tan(\pi(v'-v)) + \mathbf{r}_v^2 \tan^2(\pi(v'-v)))^{3/2}} \end{aligned}$$

With the analytically computable integrals (see appendix D)

$$\begin{aligned} K(m, n; A, B, C, a, b, c) &= \quad (\text{C.11}) \\ &= \pi \int_0^1 du \int_0^1 dv \frac{(A \tan^2(\pi u) + 2B \tan(\pi u) \tan(\pi v) + C \tan^2(\pi v)) e^{2\pi i(mu+nv)}}{(a \tan^2(\pi u) + 2 b \tan(\pi u) \tan(\pi v) + c \tan^2(\pi v))^{3/2}} \end{aligned}$$

one gets for the singular integral

$$\hat{h}_{sing}(u, v; m', n') = K(m', n'; A, B, C, \mathbf{r}_u^2, \mathbf{r}_u \cdot \mathbf{r}_v, \mathbf{r}_v^2) e^{2\pi i(m'u+n'v)} \quad (\text{C.12})$$

with  $A = (\mathbf{r}_v \times \mathbf{r}_u) \cdot \mathbf{r}_{uu}$ ,  $B = (\mathbf{r}_v \times \mathbf{r}_u) \cdot \mathbf{r}_{uv}$ ,  $C = (\mathbf{r}_v \times \mathbf{r}_u) \cdot \mathbf{r}_{vv}$ .

The regularized integral can be Fourier transformed numerically.

$$\hat{h}_{reg}(u, v; m', n') = \int_0^1 du' \int_0^1 dv' (h(u, v; u', v') - h_{sing}(u, v; u' - u, v' - v)) e^{2\pi i(m'u'+n'v')} \quad (\text{C.13})$$

For the Fourier transform of  $h(u, v; u', v')$  one gets

$$\hat{h}(u, v; m', n') = \hat{h}_{reg}(u, v; m', n') + \hat{h}_{sing}(u, v; m', n') \quad (\text{C.14})$$

## D The regularisation integrals

In appendix C a subtraction method to regularize singular Fourier integrals has been presented using the following analytically computable integrals [21],[22] :

$$I_{mn} = \pi \int_0^1 \int_0^1 du dv \frac{e^{2\pi i(mu+nv)}}{(a \tan^2(\pi u) + 2b \tan(\pi u) \tan(\pi v) + c \tan^2(\pi v))^{\frac{1}{2}}} \quad (\text{D.1})$$

and

$$K_{mn} = \pi \int_0^1 \int_0^1 du dv \frac{(A \tan^2(\pi u) + 2B \tan(\pi u) \tan(\pi v) + C \tan^2(\pi v)) e^{2\pi i(mu+nv)}}{(a \tan^2(\pi u) + 2b \tan(\pi u) \tan(\pi v) + c \tan^2(\pi v))^{\frac{3}{2}}} \quad (\text{D.2})$$

with  $ac - b^2 > 0$ . The integrals  $K_{mn}$  can be obtained by deriving the integrals  $I_{mn}$  with respect to  $a, b, c$  :

$$K_{mn} = -2(A \frac{\partial}{\partial a} + B \frac{\partial}{\partial b} + C \frac{\partial}{\partial c}) I_{mn}. \quad (\text{D.3})$$

To compute the  $I_{mn}$  a generating function  $\mathcal{I}$  is introduced:

$$\mathcal{I} = \sum_{m=0, n=0}^{\infty, \infty} I_{mn} s^m t^n. \quad (\text{D.4})$$

Summing up the power series, one obtains  $\mathcal{I}$  in closed form:

$$\mathcal{I} = \pi \int_0^1 \int_0^1 \frac{du dv}{(1 - se^{2\pi iu})(1 - te^{2\pi iv})(a \tan^2(\pi u) + 2b \tan(\pi u) \tan(\pi v) + c \tan^2(\pi v))^{\frac{1}{2}}}. \quad (\text{D.5})$$

With the variables  $(r, y) : (y = \tan \pi u, ry = \tan \pi v)$  one gets for  $\mathcal{I}$

$$\mathcal{I} = \frac{1}{4\pi} \int_{-\infty}^{+\infty} \int_{-\infty}^{+\infty} dr dy \left( \frac{1}{y+i\alpha} - \frac{1}{y-i} \right) \left( \frac{1}{ry+i\beta} - \frac{1}{ry-i} \right) \frac{1}{(a+2br+cr^2)^{\frac{1}{2}}} \quad (\text{D.6})$$

with

$$\alpha = \frac{1-s}{1+s}, \quad \beta = \frac{1-t}{1+t}. \quad (\text{D.7})$$

Integrating  $\mathcal{I}$  with respect to  $y$ , one obtains

$$\begin{aligned} \mathcal{I} &= \frac{1}{2} \int_0^{\infty} dr \left( \frac{1}{\beta+\alpha r} + \frac{1}{1+r} \right) \frac{1}{(a-2br+cr^2)^{\frac{1}{2}}} \\ &+ \frac{1}{2} \int_0^{\infty} dr \left( \frac{1}{1+\alpha r} + \frac{1}{\beta+r} \right) \frac{1}{(a+2br+cr^2)^{\frac{1}{2}}}. \end{aligned} \quad (\text{D.8})$$

and

$$\int_0^{\infty} dr \left( \frac{1}{\beta+\alpha r} \right) \frac{1}{\sqrt{a-2br+cr^2}} = \frac{1}{\gamma} \ln \frac{\alpha(\gamma\sqrt{c} + \alpha c + \beta b)}{\beta(\gamma\sqrt{a} - \alpha b - \beta a)} \quad (\text{D.9})$$

with  $\gamma = \sqrt{a\beta^2 + 2b\alpha\beta + c\alpha^2}$

With the substitution  $x : x = (1-r)/(1+r)$  the function  $\mathcal{I}$  can be written as a sum of four terms:

$$\mathcal{I} = h^+(s, t) + h^+(0, 0) + h^-(s, 0) + h^-(0, t), \quad (\text{D.10})$$

with

$$h^{\pm}(s, t) = \frac{(1+s)(1+t)}{2} \int_{-1}^{+1} \frac{dx}{(1-st - (s-t)x)(a^{\mp} + 2dx + a^{\pm}x^2)^{\frac{1}{2}}} \quad (\text{D.11})$$

and

$$\begin{aligned} a^+ &= a + 2b + c, \\ a^- &= a - 2b + c, \\ d &= c - a. \end{aligned}$$

The  $I_{mn}$  are then obtained by expanding  $\mathcal{I}$  again as a power series in  $s$  and  $t$ . One starts by expanding the functions  $h^{\pm}$

$$h^{\pm}(s, t) = \frac{1}{2} \frac{(1+s)(1+t)}{1-st} \sum_{\ell=0}^{\infty} \left( \frac{s-t}{1-st} \right)^{\ell} T_{\ell}^{\pm} \quad (\text{D.12})$$

with

$$T_\ell^\pm = \int_{-1}^{+1} dx \frac{x^\ell}{(a^\mp + 2dx + a^\pm x^2)^{\frac{1}{2}}} \quad (\text{D.13})$$

Expanding the  $h^\pm$  further, one finally obtains

$$I_{mn} = \begin{cases} c_{mn}^+ + c_{m-1n}^+ + c_{m-1}^+ + c_{m-1n-1}^+, & \text{for } m \geq 1, n \geq 1 \\ c_{m0}^+ + c_{m-10}^+ + c_{m0}^- + c_{m-10}^-, & \text{for } m \geq 1, n = 0 \\ c_{0n}^+ + c_{0n-1}^+ + c_{0n}^- + c_{0n-1}^-, & \text{for } m = 0, n \geq 1 \\ c_{00}^+ + c_{00}^- + c_{00}^- + c_{00}^-, & \text{for } m = 0, n = 0 \end{cases} \quad (\text{D.14})$$

with

$$c_{mn}^\pm = \sum_{\ell=0}^{\frac{m+n-|m-n|}{2}} \frac{(-1)^{\ell + \frac{|m-n|-m+n}{2}} \left(\frac{m+n+|m-n|}{2} + \ell\right)! T_{|m-n|+2\ell}^\pm}{2 \left(\frac{m+n-|m-n|}{2} - \ell\right)! (|m-n| + \ell)! \ell!}.$$

The integrals  $T_\ell^\pm$  can be calculated by using a recurrence relation

$$\begin{aligned} T_0^\pm &= \frac{1}{\sqrt{a^\pm}} \log \frac{\sqrt{c a^\pm} + c \pm b}{\sqrt{a a^\pm} - a \mp b}, \\ T_1^\pm &= \frac{1}{a^\pm} (2(\sqrt{c} - \sqrt{a}) - (c - a)T_0^\pm), \\ T_\ell^\pm &= \frac{1}{\ell a^\pm} (2(\sqrt{c} + (-1)^\ell \sqrt{a}) - (2\ell - 1)(c - a)T_{\ell-1}^\pm - (\ell - 1) a^\mp T_{\ell-2}^\pm) \quad \text{for } \ell \geq 2. \end{aligned} \quad (\text{D.15})$$

The Fourier integrals  $K_{mn}$  follow from the  $I_{mn}$  by differentiation. One gets the same formulas (D.14) as for the  $I_{mn}$  replacing the integrals  $T_\ell^\pm$  by the integrals  $S_\ell^\pm$ , which are given by

$$S_\ell^\pm = \int_{-1}^{+1} dx x^\ell \frac{(A^\mp + 2Dx + A^\pm x^2)}{(a^\mp + 2dx + a^\pm x^2)^{\frac{3}{2}}} \quad (\text{D.16})$$

with

$$\begin{aligned} A^+ &= A + 2B + C, \\ A^- &= A - 2B + C, \\ D &= C - A. \end{aligned}$$

As for the  $T_\ell^\pm$ , recurrence formulas can be derived for the  $S_\ell^\pm$ , but the  $S_\ell^\pm$  can also be



expressed in terms of the  $T_\ell^\pm$  by appropriate partial integration. One obtains for  $S_\ell^+$

$$\begin{aligned}
& (a + 2b + c)(ac - b^2)S_\ell^+ = \\
& \left( (A + 2B + C)(ac - b^2) + \ell(k_1(a + 2b + c) + k_2(c - a)) \right) T_\ell^+ \\
& + \ell(k_1(c - a) + k_2(a - sb + c)) T_{\ell-1}^+ \\
& - \frac{(c + b)k_1 + (c - b)k_2}{\sqrt{c}} - (-1)^\ell \frac{(a + b)k_1 - (a - b)k_2}{\sqrt{a}}
\end{aligned} \tag{D.17}$$

with

$$\begin{aligned}
k_1 &= (a + c)B - (A + C)b, \\
k_2 &= C(a + b) - B(c - a) - A(c + b).
\end{aligned}$$

The formula for  $S_\ell^-$  is obtained by replacing  $b$  by  $-b$  and  $B$  by  $-B$ , and  $T_\ell^+, T_{\ell-1}^+$  by  $T_\ell^-, T_{\ell-1}^-$ .

The forward computation of the recurrence relation  $T_\ell^+$  gets unstable if  $b < 0$ , and for  $T_\ell^-$  if  $b > 0$  [32]. Considering the homogeneous equation

$$\mathcal{L}[T_\ell^+] \equiv T_{\ell+2}^+ + \frac{(2\ell + 3)d}{(\ell + 2)a^+} T_{\ell+1}^+ + \frac{(\ell + 1)a^-}{(\ell + 2)a^+} T_\ell^+ = 0 \tag{D.18}$$

with the ansatz  $T_\ell^+ \approx t^\ell$  one gets the characteristic equation

$$t^2 + \frac{(2\ell + 3)d}{(\ell + 2)a^+} t + \frac{(\ell + 1)a^-}{(\ell + 2)a^+} = 0 \tag{D.19}$$

with the solution for large  $\ell \rightarrow \infty$

$$t_\pm = -\frac{d}{a^+} \pm i \frac{\sqrt{a c - b^2}}{a^+} \text{ and } |t_\pm| = \frac{a^-}{a^+} \tag{D.20}$$

For  $b < 0$  the moduli are  $|t_\pm| > 1$  so that the forward recursion is unstable. In that case the  $T_\ell^+$  can be obtained by solving the recurrence relation in the backward direction. First one generates a solution of the nonhomogeneous equation by using the equation in the backward direction with starting values

$$z_N(N + 1) = z_N(N) = 0.$$

Then one generates a solution  $y_N(\ell)$  of the homogeneous equation  $\mathcal{L}[y(\ell)] = 0$  by using the equation in the backward direction with

$$y_N(N + 1) = 0, \quad y_N(N) = 1.$$

Then the solution  $w_N(\ell)$  is obtained by

$$w_N(\ell) = \lambda(N) y_N(\ell) + z_N(\ell), \quad 0 \leq \ell \leq N + 1 \quad (\text{D.21})$$

with

$$\lambda(N) = \frac{T_0^+ - z_N(0)}{y_N(0)}$$

For  $N \rightarrow \infty$  the  $w_N(\ell)$  converges to  $T_\ell^+$ .

For large values of  $m, n$  an asymptotic expansion for the Fourier integral (D.1)

$$I_{mn} = \pi \int_{-\frac{1}{2}}^{\frac{1}{2}} \int_{-\frac{1}{2}}^{\frac{1}{2}} du dv \frac{e^{2\pi i(mu+nv)}}{(a \tan^2(\pi u) + 2b \tan(\pi u) \tan(\pi v) + c \tan^2(\pi v))^{\frac{1}{2}}}, \quad (\text{D.22})$$

can be derived.

With the substitution

$$\pi u = r \cos \varphi, \quad \pi v = r \sin \varphi$$

and

$$m = \lambda \cos \varphi_0, \quad n = \lambda \sin \varphi_0, \quad \lambda^2 = m^2 + n^2 \quad (\text{D.23})$$

one gets

$$I_{mn} = \int_0^{2\pi} d\varphi \int_0^{R(\varphi)} dr g(r, \varphi) e^{i\lambda f(r, \varphi)} \quad (\text{D.24})$$

with

$$\begin{aligned} f(r, \varphi) &= 2r \cos(\varphi - \varphi_0) \\ g(r, \varphi) &= \frac{r}{\pi(a \tan^2(r \cos \varphi) + 2b \tan(r \cos \varphi) \tan(r \sin \varphi) + c \tan^2(r \sin \varphi)^{1/2})} \end{aligned}$$

and

$$R(\varphi) = \left\{ \begin{array}{ll} \frac{1}{2|\cos(\varphi)|} & \text{for } |\varphi - l\pi/2| < \pi/4 \quad l = 0, 2 \\ \frac{1}{2|\sin(\varphi)|} & l = 1, 3 \end{array} \right\}$$

The procedure used is based on the method given in [33]. In the present case the main contribution to the asymptotic expansion comes from the stationary point, where the derivatives  $\frac{\partial}{\partial r} f(r, \varphi) = 0$ ,  $\frac{\partial}{\partial \varphi} f(r, \varphi) = 0$  vanish. The stationary point is found to be

$$\begin{aligned} r &= 0, \\ \cos(\varphi - \varphi_0) &= 0 \rightarrow \varphi - \varphi_0 = \frac{\pi}{2}. \end{aligned} \quad (\text{D.25})$$

Defining  $\varphi' : \varphi' = \varphi - \varphi_0 - \frac{\pi}{2}$  one gets with  $\hat{g}(r, \varphi') = g(r, \varphi)$  and  $\hat{f}(r, \varphi') = f(r, \varphi)$

$$I_{mn} = \int_{-R}^R dr \int_{-\frac{\pi}{2}}^{\frac{\pi}{2}} d\varphi' \hat{g}(r, \varphi') e^{2i\lambda r \sin(\varphi')} \quad (\text{D.26})$$

with

$$\hat{g}(r, \varphi') = \frac{r}{\pi(a \tan^2(r \sin(\varphi' + \varphi_0)) - 2b \tan(r \sin(\varphi' + \varphi_0)) \tan(r \cos(\varphi' + \varphi_0)) + c \tan^2(r \cos(\varphi' + \varphi_0)))^{1/2}}$$

There has been made use of the fact that  $\hat{g}(-r, \varphi) = -\hat{g}(r, \varphi)$  and  $\hat{g}(r, \varphi + \pi) = \hat{g}(r, \varphi)$ . For  $R$  it is sufficient to choose  $R > 0$  small but finite.

Substituting  $\varphi'$  by  $t = \sin(\varphi)$  one gets

$$I_{mn} = \int_{-R}^R dr \int_{-1}^1 dt G(r, t) e^{2i\lambda r t} \quad (\text{D.27})$$

with

$$G(r, t) = \frac{r}{\pi(1 - t^2)^{1/2}(a \tan^2(rT_s) - 2b \tan(rT_s) \tan(rT_c) + c \tan^2(rT_c))^{1/2}}$$

and

$$\begin{aligned} T_s &= t \cos \varphi_0 + \sqrt{1 - t^2} \sin \varphi_0, \\ T_c &= -t \sin \varphi_0 + \sqrt{1 - t^2} \cos \varphi_0. \end{aligned} \quad (\text{D.28})$$

Substituting  $r = x - y$ ,  $t = x + y$  one gets

$$I_{mn} = 2 \int dx \int dy G(x - y, x + y) e^{2i\lambda(x^2 - y^2)}. \quad (\text{D.29})$$

The asymptotic expansion obtained for this case in [33] is given by

$$\begin{aligned} I_{mn} &= -2\pi \sum_{\nu=0}^{\nu_{max}} c_\nu e^{i\frac{\pi}{2}\nu} \frac{\nu!}{(2\lambda)^{\nu+1}}, \quad c_\nu = \sum_{j=0}^{\nu} F_{2j, 2(\nu-j)} C_{j, \nu-j} \\ C_{j, \ell} &= \frac{(-1)^{\ell+1}}{2^{2j+1}} \binom{2j}{j} \frac{1 \cdot 3 \cdots (2\ell - 1)}{(2\ell + 2j)(2\ell + 2j - 2) \cdots (2j + 2)} \\ F_{i, k} &= \frac{1}{i!} \frac{1}{k!} \left[ \frac{\partial^i}{\partial x^i} \frac{\partial^k}{\partial x^k} G(x - y, x + y) \right]_{\substack{x=0 \\ y=0}} \end{aligned} \quad (\text{D.30})$$

The coefficients  $C_{j,\nu-j}$  can be written also in closed form

$$C_{j,\nu-j} = \frac{(-1)^{\nu-j+1} (2j)! Z}{2^{2j+1} j! j! N}, \quad Z = \frac{(2\nu-2j)!}{2^{\nu-j}(\nu-1)!}, \quad N = \frac{2^{\nu-j}\nu!}{j!} \quad (\text{D.31})$$

so that one finds

$$I_{mn} = \sum_{\nu=0}^{\nu_{max}} \frac{4\pi e^{i\nu\pi/2}}{\nu! (2\lambda)^{\nu+1}} \sum_{j=0}^{\nu} \frac{(-1)^{\nu-j}}{2^{2\nu+1}} \frac{\nu!}{j! (\nu-j)!} \frac{\partial^{2j}}{\partial x^{2j}} \frac{\partial^{2(\nu-j)}}{\partial y^{2(\nu-j)}} G(x-y, x+y) \quad (\text{D.32})$$

or

$$I_{mn} = \sum_{\nu=0}^{\nu_{max}} \frac{4\pi}{\nu! (2\lambda)^{\nu+1}} e^{i\nu\pi/2} \frac{1}{2^{2\nu+1}} \left( \frac{\partial^2}{\partial x^2} - \frac{\partial^2}{\partial y^2} \right)^\nu G(x-y, x+y)$$

or

$$I_{mn} = \sum_{\nu=0}^{\nu_{max}} \frac{4\pi}{\nu! (2\lambda)^{\nu+1}} e^{i\nu\pi/2} \frac{1}{2^{2\nu+1}} \left[ \left( \left( \frac{\partial}{\partial r} + \frac{\partial}{\partial t} \right)^2 - \left( -\frac{\partial}{\partial r} + \frac{\partial}{\partial t} \right)^2 \right)^\nu G(r, t) \right]_{\substack{r=0 \\ t=0}}$$

and finally

$$I_{mn} = \sum_{\nu=0}^{\nu_{max}} \frac{2\pi e^{i\nu\pi/2}}{\nu! (2\lambda)^{\nu+1}} \left[ \left( \frac{\partial}{\partial r} \frac{\partial}{\partial t} \right)^\nu G(r, t) \right]_{\substack{r=0 \\ t=0}}. \quad (\text{D.33})$$

The two leading terms of the asymptotic expansion are given by

$$I_{mn} = \pi \left[ \frac{G(r, t)}{\lambda} - \frac{G(r, t)_{rrtt}}{8\lambda^3} \right]_{\substack{r=0 \\ t=0}} \quad (\text{D.34})$$

Here it has been made use of the fact that  $G(r, t)$  is a function of  $r^2$ , so that uneven derivatives vanish for  $r = 0$ .

Expanding  $G(r, t)$  at  $r = 0, t = 0$  up to second order in  $r$  and  $t$  one gets

$$\begin{aligned} G(r, t) &= \frac{1}{\pi \sqrt{(1-t^2)(\alpha(t) + \beta(t) r^2)}}, \\ \alpha(t) &= a T_s^2 - 2b T_s T_c + c T_c^2, \\ \beta(t) &= \frac{2}{3} (a T_s^4 - b (T_s T_c^3 + T_c T_s^3) + c T_c^4). \end{aligned} \quad (\text{D.35})$$

Using (D.28) one gets for  $\alpha(t)$  and  $\beta(t)$  up to second order in  $t$

$$\alpha(t) = a_0 + a_1 t + a_2 t^2, \quad \beta(t) = b_0 + b_1 t + b_2 t^2, \quad (\text{D.36})$$

where the coefficients  $a_i, b_i, i = 0, 1, 2$  depend only on the  $m, n$ -harmonics (D.23)

$$\cos \varphi_0 = \frac{m}{\lambda}, \quad \sin \varphi_0 = \frac{n}{\lambda}, \quad \lambda = \sqrt{m^2 + n^2},$$

and are given by

$$\begin{aligned}
a_0 &= a \sin^2(\varphi_0) - 2b \sin(\varphi_0) \cos(\varphi_0) + c \cos^2(\varphi_0), \\
a_1 &= (a - c) \sin(2\varphi_0) - 2b \cos(2\varphi_0), \\
a_2 &= (a - c) \cos(2\varphi_0) + 2b \sin(2\varphi_0), \\
b_0 &= \frac{2}{3}(a \sin^4(\varphi_0) - b \sin(\varphi_0) \cos(\varphi_0) + c \cos^4(\varphi_0)), \\
b_1 &= \frac{2}{3}(2(a \sin^2(\varphi_0) - c \cos^2(\varphi_0)) \sin(2\varphi_0) - b \cos(2\varphi_0)), \\
b_2 &= (a + c) \sin^2(2\varphi_0) - \frac{4}{3}(a \sin^4(\varphi_0) + c \cos^4(\varphi_0)) + \frac{2}{3}b \sin(2\varphi_0).
\end{aligned} \tag{D.37}$$

For the two leading terms of the asymptotic expansion one obtains

$$I_{mn} = \frac{1}{\lambda} \frac{1}{\sqrt{a_0}} + \frac{1}{8\lambda^3} \left( \frac{b_0 + 2b_2}{\sqrt{a_0}^3} - 3 \frac{a_2 b_0 + a_1 b_1}{\sqrt{a_0}^5} + \frac{15}{4} \frac{a_1^2 b_0}{\sqrt{a_0}^7} \right) \tag{D.38}$$

The asymptotic expansion of  $K_{mn}$  (D.2) can be obtained from  $I_{mn}$  using (D.3)

$$\begin{aligned}
K_{mn} &= \frac{1}{\lambda} \frac{A_0}{\sqrt{a_0}^3} + \frac{3A_0}{8\lambda^3} \left( \frac{b_0 + 2b_2}{\sqrt{a_0}^5} - 5 \frac{a_2 b_0 + a_1 b_1}{\sqrt{a_0}^7} + \frac{35}{4} \frac{a_1^2 b_0}{\sqrt{a_0}^9} \right) \\
&- \frac{1}{4\lambda^3} \left( \frac{B_0 + 2B_2}{\sqrt{a_0}^3} - 3 \frac{A_2 b_0 + a_2 B_0 + A_1 b_1 + a_1 B_1}{\sqrt{a_0}^5} + \frac{15}{4} \frac{2a_1 A_1 b_0 + a_1^2 B_0}{\sqrt{a_0}^7} \right)
\end{aligned} \tag{D.39}$$

where the expressions for  $A_i, B_i, i = 0, 1, 2$  are obtained from (D.37) by replacing  $a, b, c$  by  $A, B, C$ .